

Solid-State NMR of Quadrupolar Nuclei

A photograph of the Columbus, Ohio skyline at dusk or night. The city lights reflect off the surface of the Scioto River in the foreground. A paved path or boardwalk runs along the riverbank in the lower-left foreground. The buildings in the background are illuminated, with the Terminal Tower being particularly prominent.

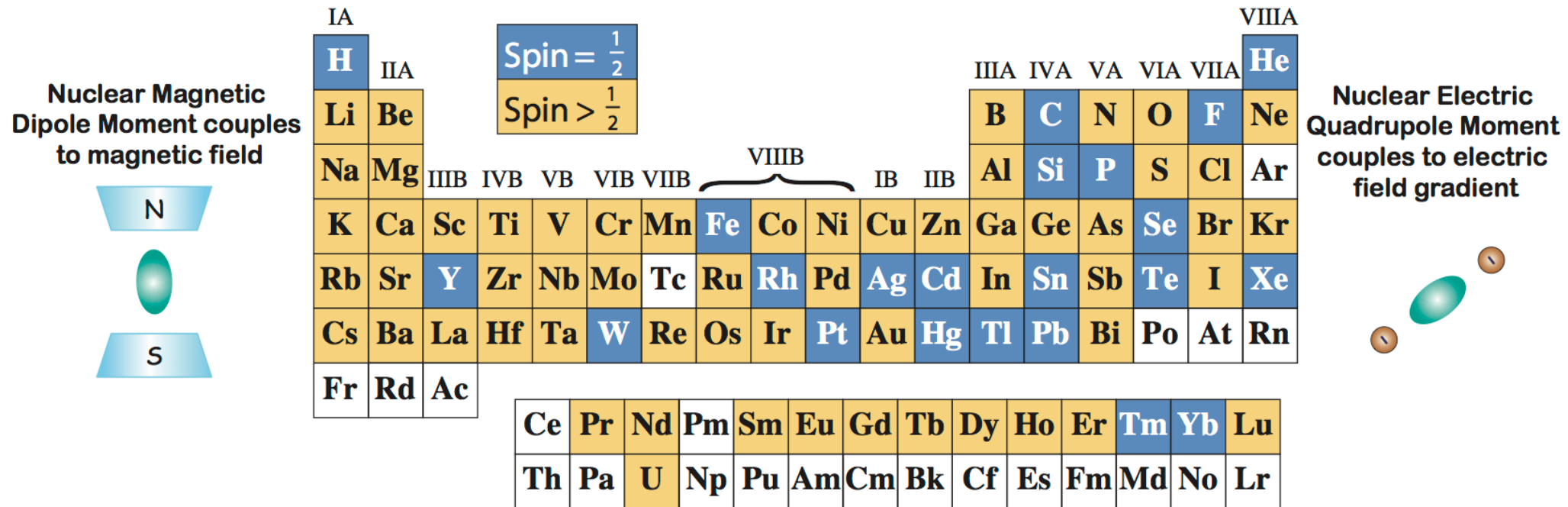
Philip J. Grandinetti
Ohio State University
Columbus, OH, USA

<http://www.grandinetti.org>

Tutorial Lecture presented at
NMR Winter School
Stowe, Vermont
January 2013

The Big Picture

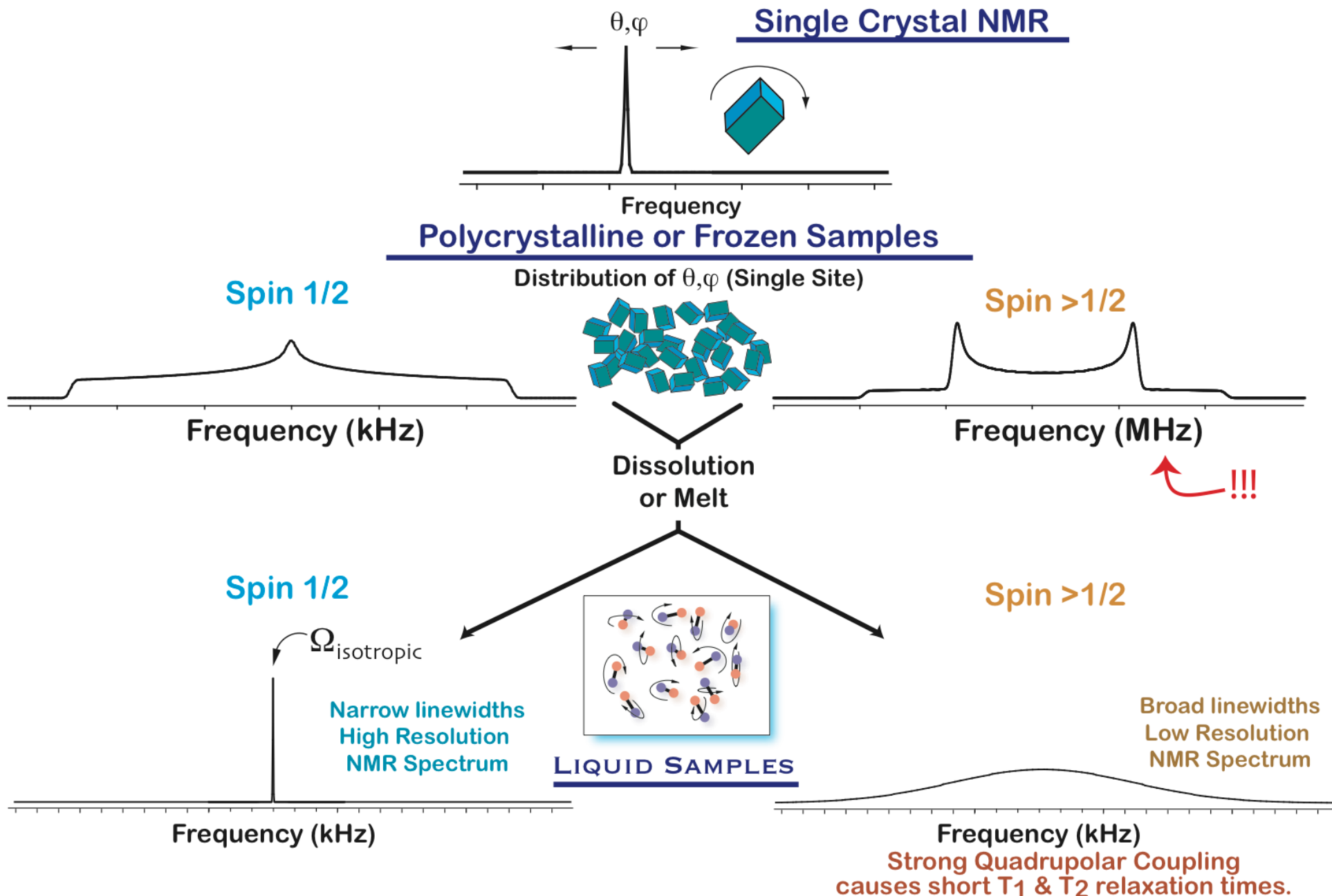
Most Nuclei have Electric quadrupole moments



	$l = 0$	$l = 1$	$l = 2$	$l = 3$	$l = 4$
SPIN	monopole	dipole	quadrupole	octapole	hexadecapole
$I = 0$	electric	0	0	0	0
$I = \frac{1}{2}$	electric	magnetic	0	0	0
$I = 1$	electric	magnetic	electric	0	0
$I = \frac{3}{2}$	electric	magnetic	electric	magnetic	0
$I = 2$	electric	magnetic	electric	magnetic	electric

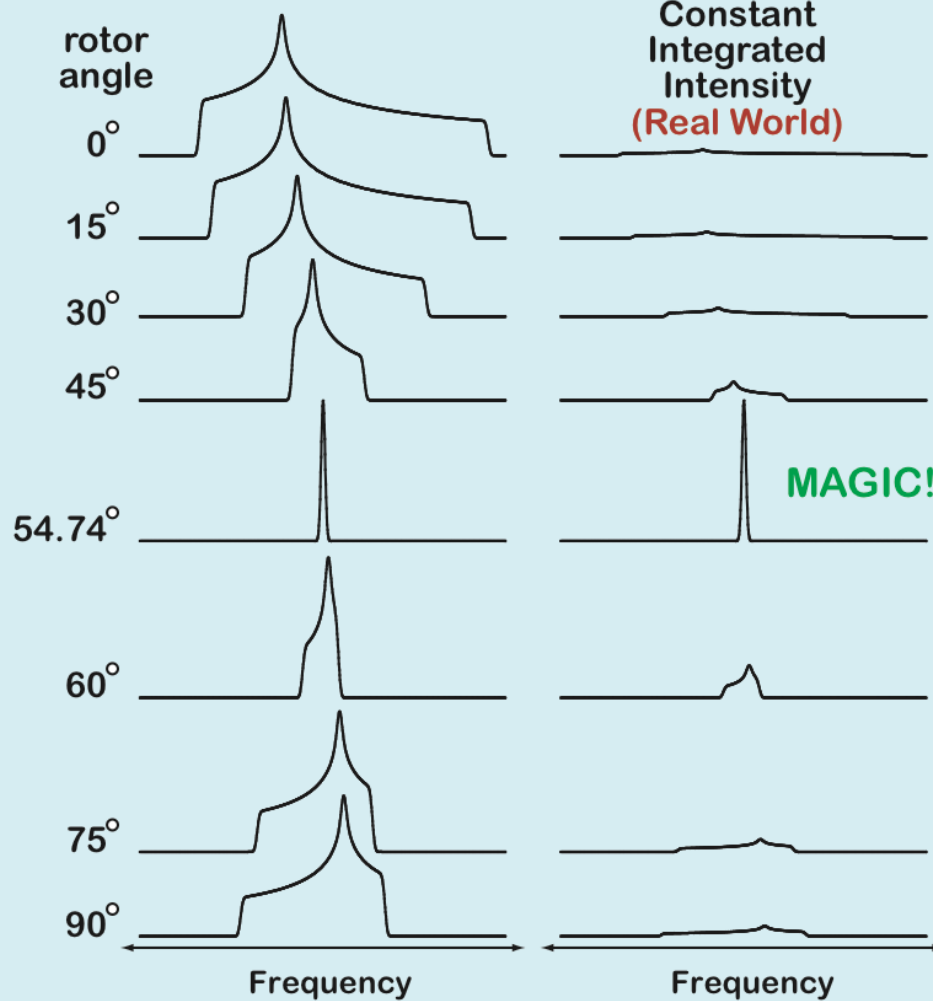
NMR of Quadrupolar Nuclei

What's the Problem?

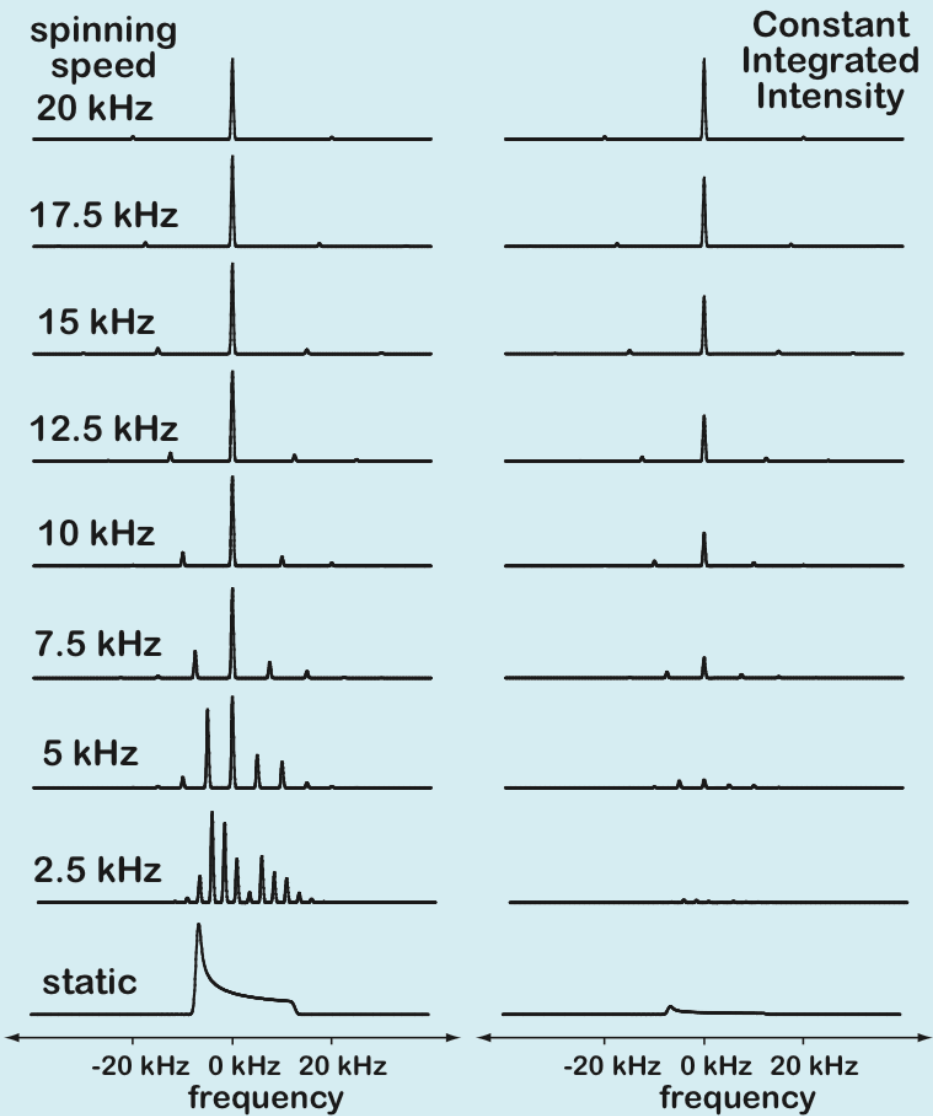


MAS eliminates 1st Order Anisotropies

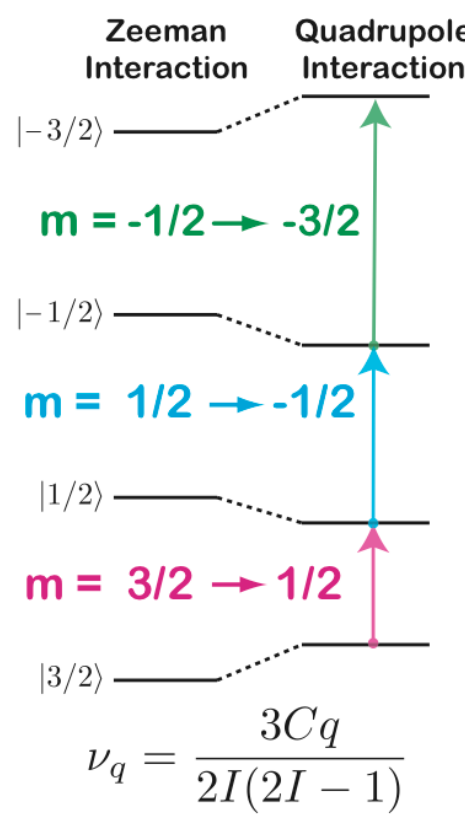
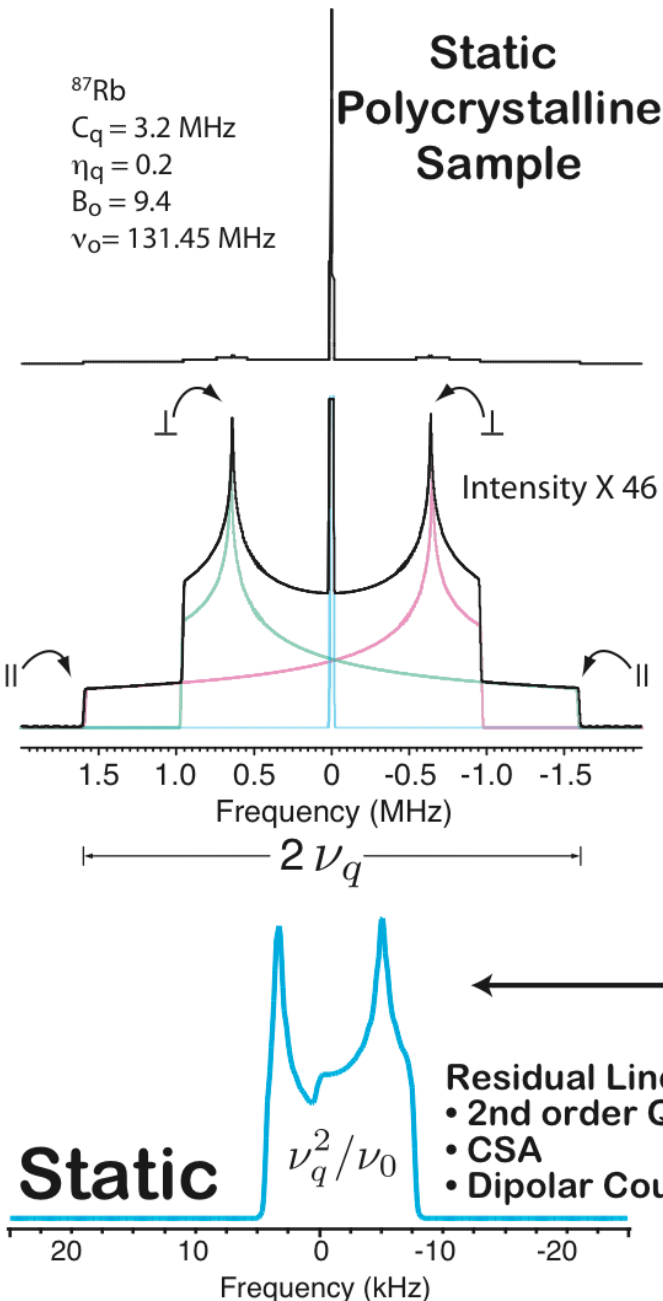
Variable-Angle Spinning Spectra as a function of angle



Magic-Angle Spinning Spectra as a function of spinning speed

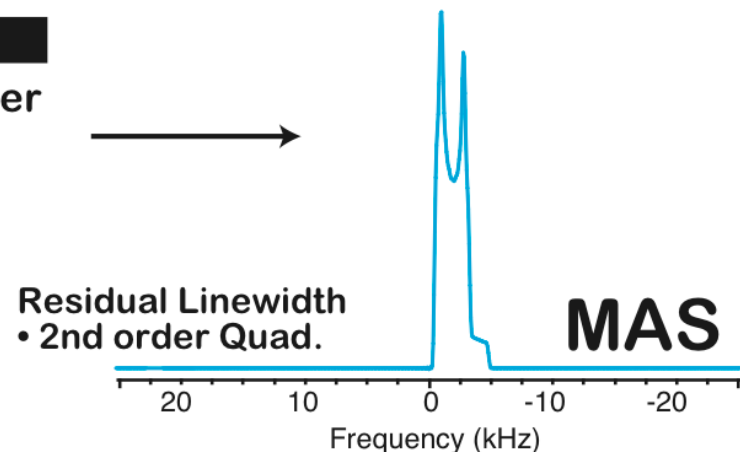
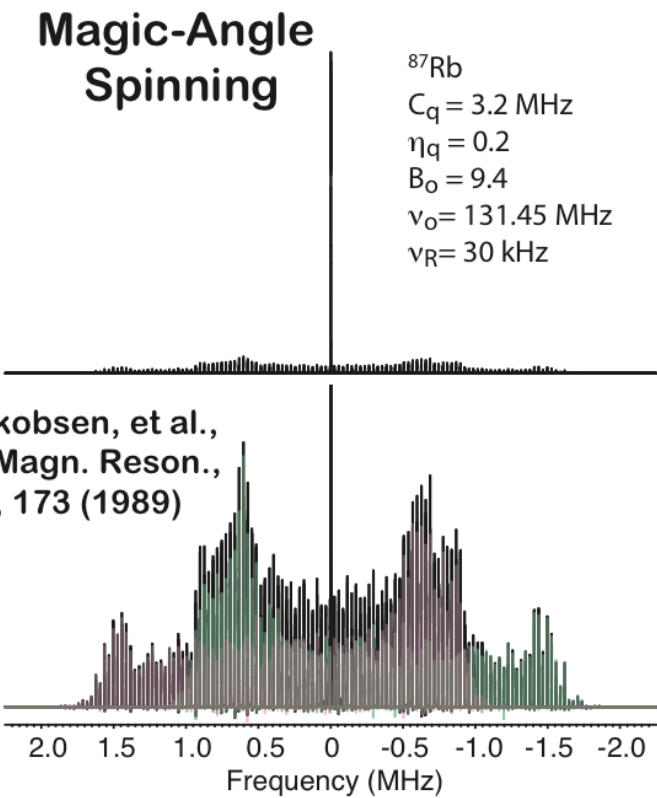


Quadrupolar Nuclei have a Narrow Central Transition but MAS is Inadequate

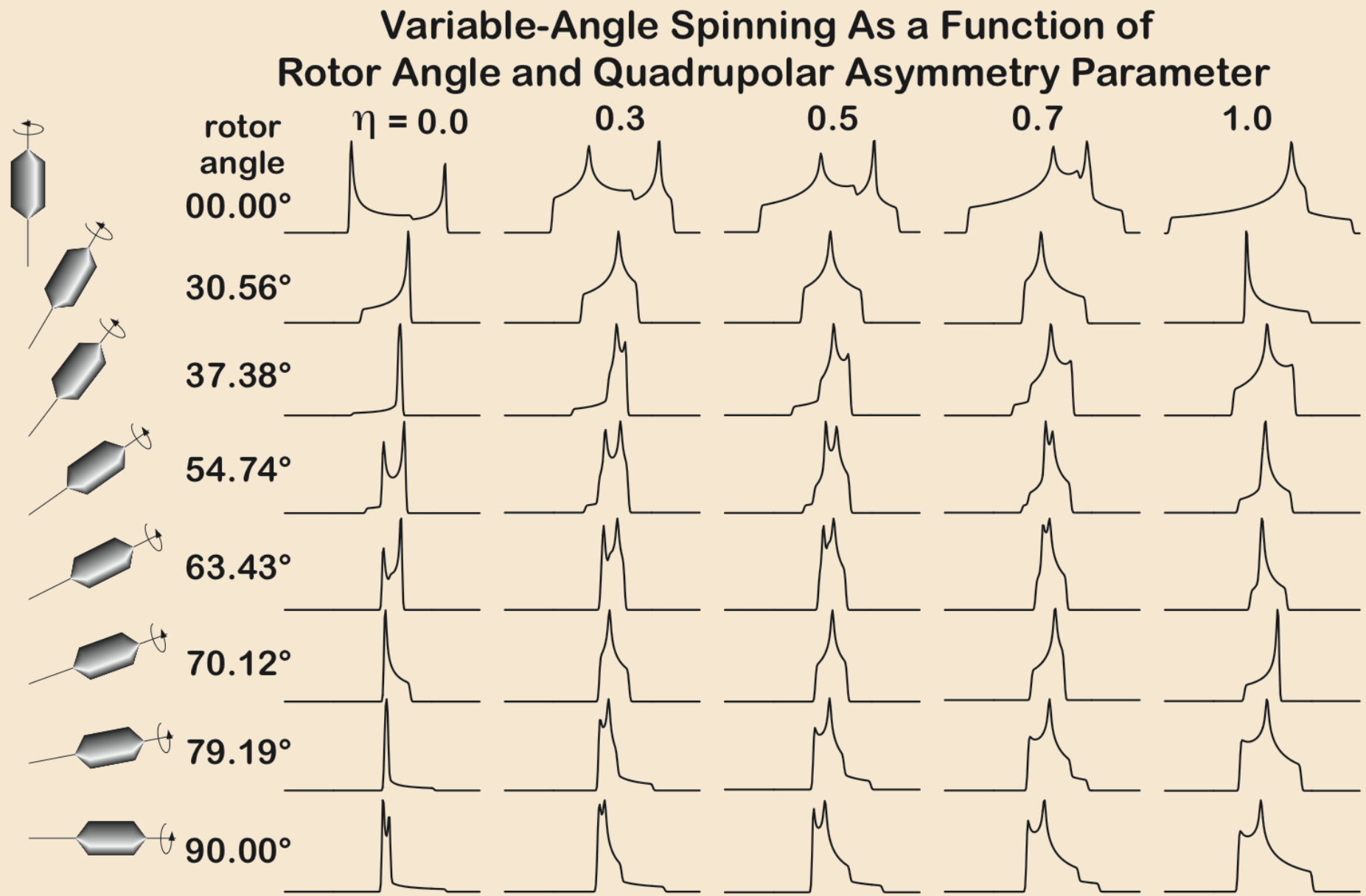


Central Transition
 Unaffected by First Order
 Quadrupolar splitting
 $m = 1/2 \rightarrow -1/2$

- Residual Linewidth
 • 2nd order Quad.
 • CSA
 • Dipolar Couplings



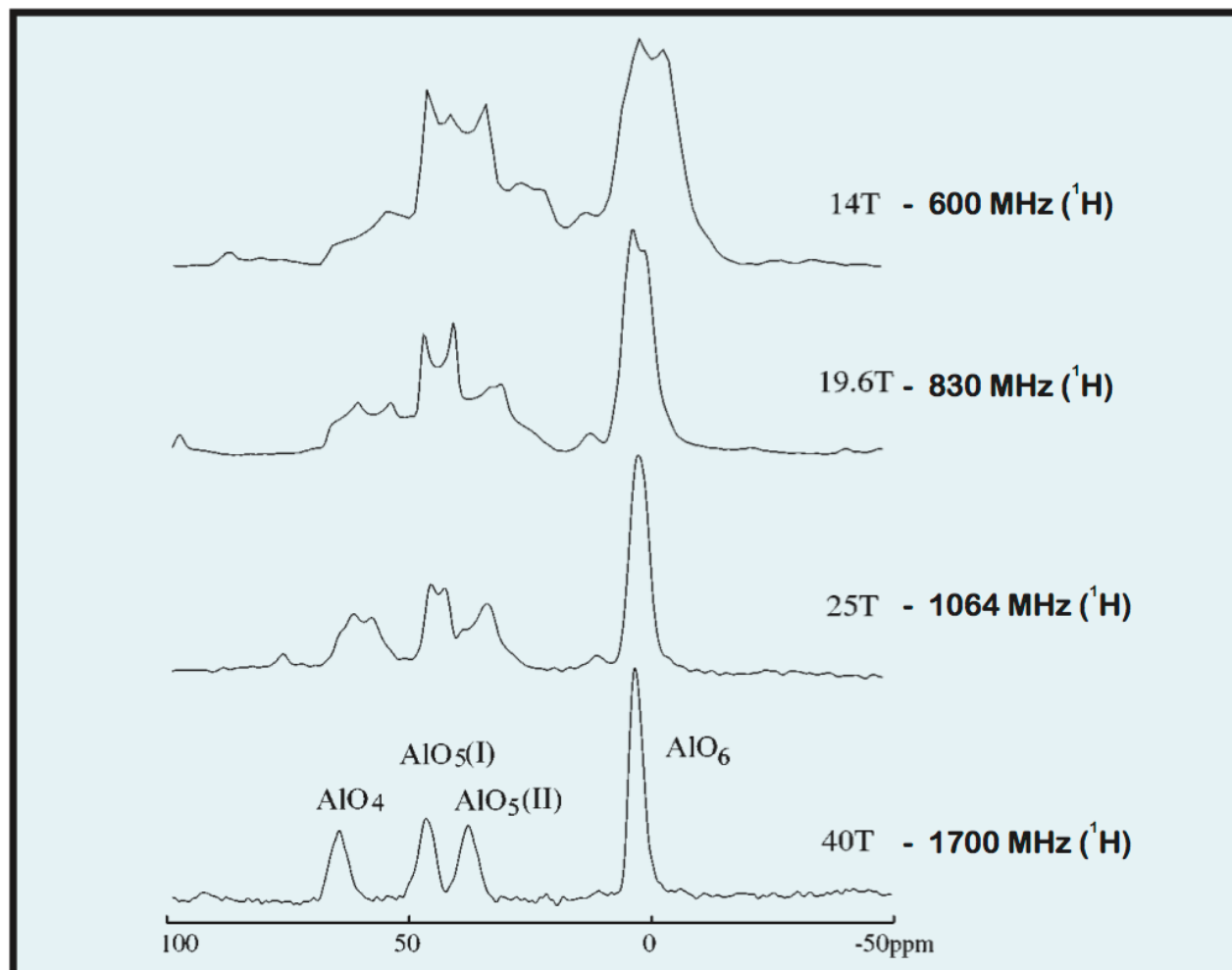
Variable Angle Spinning: Central Transition of Quadrupolar Nuclei



One Solution: Really High magnetic fields

2nd-order anisotropies are inversely proportional to magnetic field strength

^{27}Al CT MAS spectra of aluminoborate $9\text{Al}_2\text{O}_3 + 2\text{B}_2\text{O}_3$ (A_9B_2) compound from 14 to 40 T.



**We've got no money,
so we've got to think.**

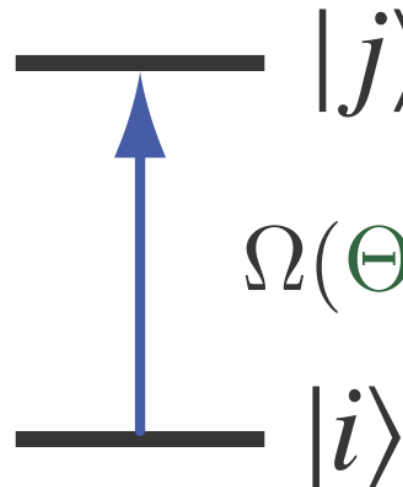
Ernest Rutherford

How are 2nd-order anisotropies different from 1st-order anisotropies?

see also

“Symmetry Pathways in Solid-State NMR”
Grandinetti, Ash, Trease,
Prog. NMR Spect.
59, 121 (2001)

NMR Transition Frequency is Sum of Components



$$\Omega(\Theta, i, j) = \sum_k \Omega_k(\Theta, i, j)$$

and each component is the product of three terms:

$$\Omega_k(\Theta, i, j) = \omega_k \cdot \Xi_L^{(k)}(\Theta) \cdot \xi_l^{(k)}(i, j)$$

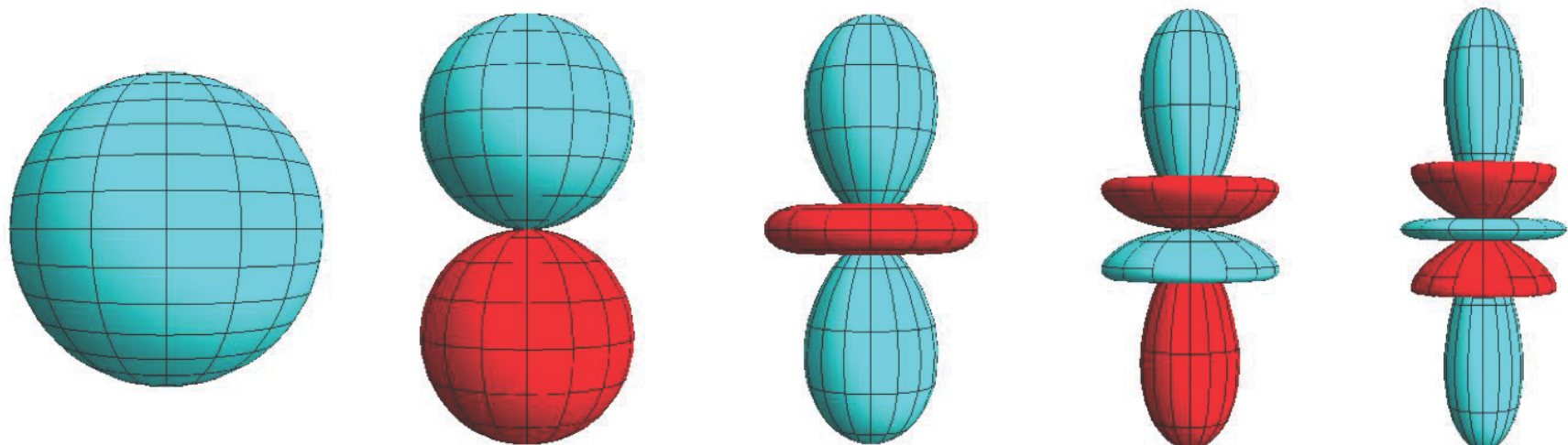
Component
Strength Spatial
Function

Spin
Transition
Function

Relabel spatial function for each rank of L

$$\Xi_L^{(k)}(\Theta) \propto R_{L,0}^{(k)}(\Theta)$$

$L =$	$\Xi_L(\Theta)$	0	1	2	3	4
	S, $P(\Theta), D(\Theta), F(\Theta), G(\Theta), \dots$					



Relabel transition function for each rank of l

$$\xi_l^{(k)}(i, j) \propto \langle j | \hat{T}_{l,0}^{(k)} | j \rangle - \langle i | \hat{T}_{l,0}^{(k)} | i \rangle$$

$\xi_l(i, j)$			
$l = 0$	1	2	3
$s,$	$p(i, j),$	$d(i, j),$	$f(i, j), \dots$

Form of transition function depends on spin system

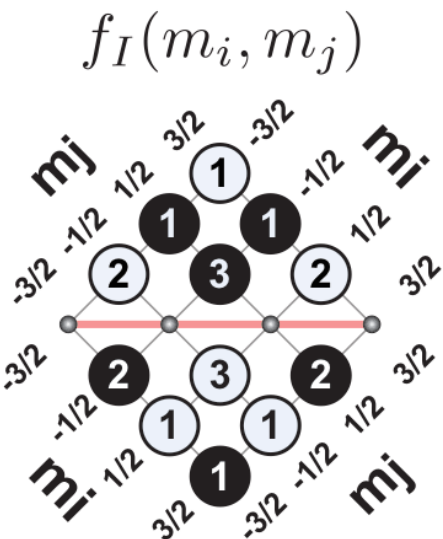
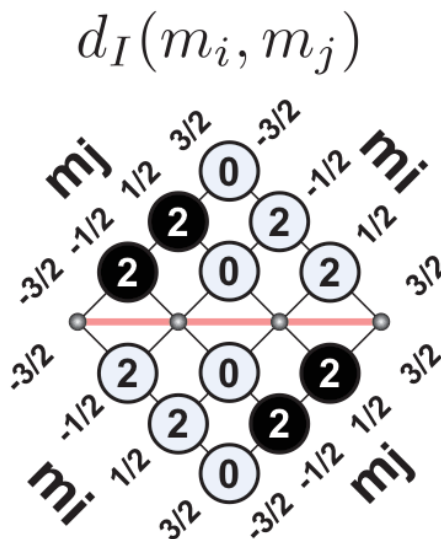
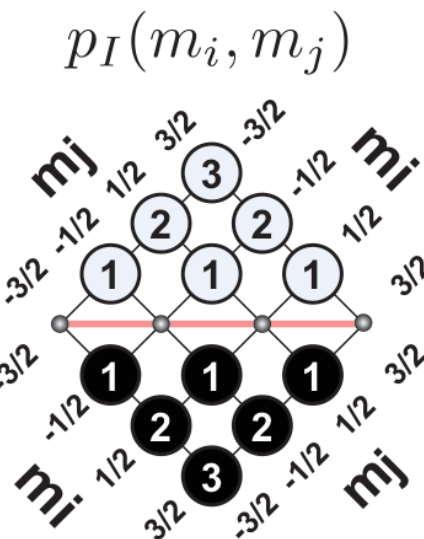
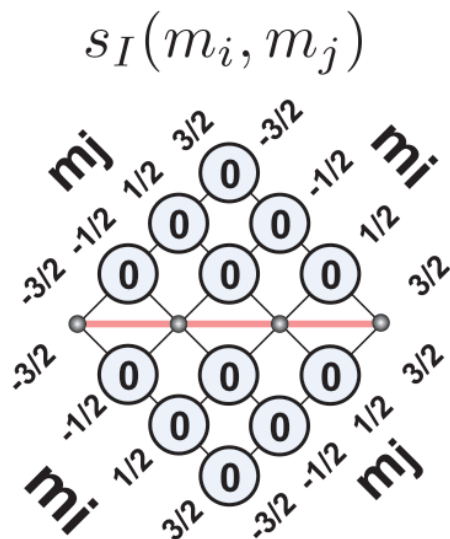
Transition function for single spin, I

$$s_I(m_i, m_j) = \quad \quad \mathbb{s}_I(m_i, m_j) = 0,$$

$$p_I(m_i, m_j) = \quad \quad \mathbb{p}_I(m_i, m_j) = m_j - m_i,$$

$$d_I(m_i, m_j) = \sqrt{\frac{2}{3}} \mathbb{d}_I(m_i, m_j) = m_j^2 - m_i^2,$$

$$f_I(m_i, m_j) = \sqrt{\frac{10}{9}} \mathbb{f}_I(m_i, m_j) = \frac{1}{3} \left[5(m_j^3 - m_i^3) + (1 - 3I(I+1))(m_j - m_i) \right]$$



Transition functions for a Spin $I=3/2$ Nucleus
Values inside solid black circles are negative

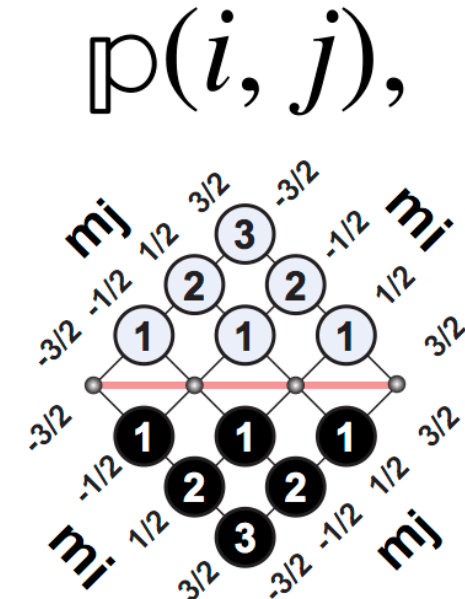
Rewrite Frequency Contributions using Symmetry Functions

First-Order Nuclear Shielding

$$\Omega_{\sigma}^{(1)} = -\omega_0 \sigma_{iso} [S^{\{\sigma\}} \cdot p_I(m_i, m_j)] - \omega_0 \zeta_{\sigma} [D^{\{\sigma\}}(\Theta) \cdot p_I(m_i, m_j)]$$

spatial function transition function

Isotropic contribution contains the **S** spatial function.

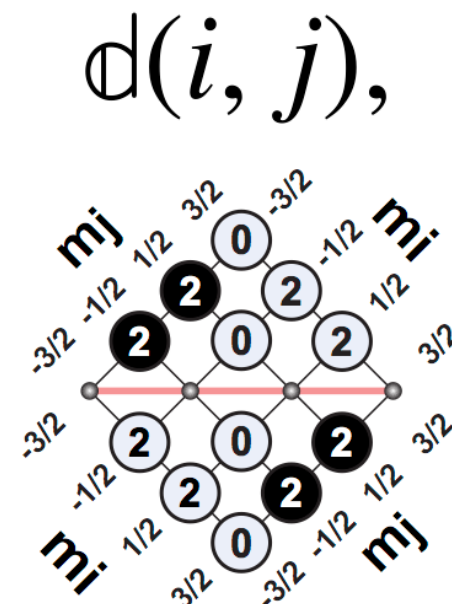


First-Order Quadrupole Coupling

$$\Omega_q^{(1)} = \omega_q [D^{\{q\}}(\Theta) \cdot d_I(m_i, m_j)]$$

Notice: d_I vanishes for all m to $-m$ transitions

$$d_I(m, -m) = 0$$



Second-Order Quadrupole Frequencies

after lengthy derivation...

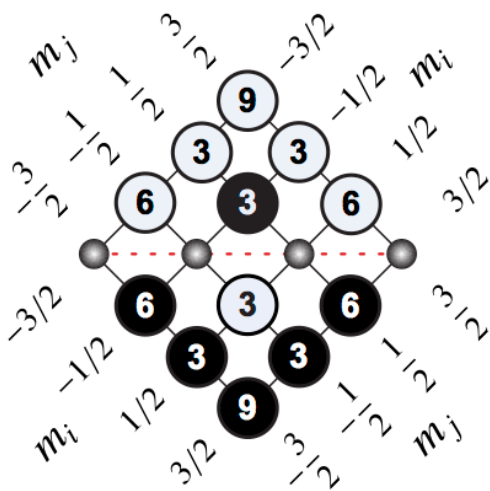
$$\Omega_q^{(2)} = \frac{\omega_q^2}{\omega_0} [\mathbb{S}^{\{qq\}} \cdot \mathbb{C}_0(m_i, m_j)] + \frac{\omega_q^2}{\omega_0} [\mathbb{D}^{\{qq\}}(\Theta) \cdot \mathbb{C}_2(m_i, m_j)] + \frac{\omega_q^2}{\omega_0} [\mathbb{G}^{\{qq\}}(\Theta) \cdot \mathbb{C}_4(m_i, m_j)]$$

Notice: All 2nd-order frequency contributions are inversely proportional to magnetic field strength

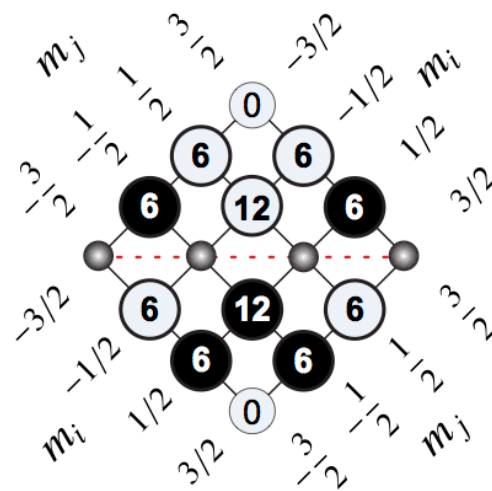
c_L are linear combinations of p_I and f_I ,

$$\mathbb{C}_L(m_i, m_j) = \pi_{L,1}^{\{2,2\}} \cdot \mathbb{P}_I(m_i, m_j) + \pi_{L,3}^{\{2,2\}} \cdot \mathbb{F}_I(m_i, m_j)$$

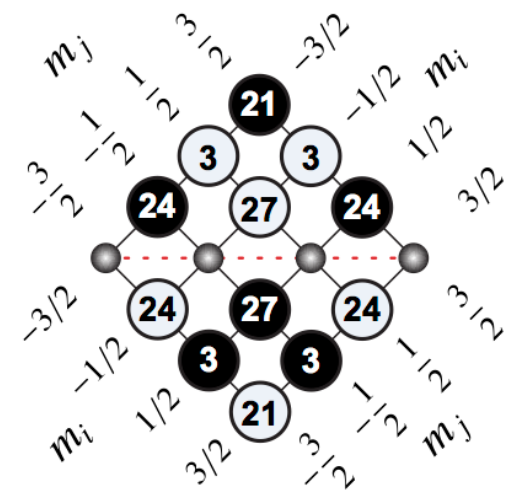
c_L transition tables for spin 3/2



$c_0(m_i, m_j)$



$c_2(m_i, m_j)$



$c_4(m_i, m_j)$

Values inside solid black circles are negative

Quadrupolar NMR Frequency Contributions

1st-Order Nuclear Shielding (a few kHz)

$$\Omega_{\sigma}^{(1)} = -\omega_0 \sigma_{iso} [\mathbb{S}^{\{\sigma\}} \cdot \mathbb{p}_I(m_i, m_j)] - \omega_0 \zeta_{\sigma} [\mathbb{D}^{\{\sigma\}}(\Theta) \cdot \mathbb{p}_I(m_i, m_j)]$$

1st-Order Quadrupolar (a few MHz)

$$\Omega_q^{(1)} = \omega_q [\mathbb{D}^{\{q\}}(\Theta) \cdot \mathbb{d}_I(m_i, m_j)]$$

2nd-Order Quadrupolar (a few kHz)

$$\Omega_q^{(2)} = \frac{\omega_q^2}{\omega_0} [\mathbb{S}^{\{qq\}} \cdot \mathbb{C}_0(m_i, m_j)] + \frac{\omega_q^2}{\omega_0} [\mathbb{D}^{\{qq\}}(\Theta) \cdot \mathbb{C}_2(m_i, m_j)] + \frac{\omega_q^2}{\omega_0} [\mathbb{G}^{\{qq\}}(\Theta) \cdot \mathbb{C}_4(m_i, m_j)]$$

All **Isotropic contributions** contain the **S** spatial function.

Need to eliminate all **anisotropic contributions** to get high resolution spectra

- Only excite m to -m transitions, so $\mathbb{d}_I(m, -m) = 0$

1st-Order Nuclear Shielding (a few kHz)

$$\Omega_{\sigma}^{(1)} = -\omega_0 \sigma_{iso} [\mathbb{S}^{\{\sigma\}} \cdot \mathbb{p}_I(m_i, m_j)] - \omega_0 \zeta_{\sigma} [\mathbb{D}^{\{\sigma\}}(\Theta) \cdot \mathbb{p}_I(m_i, m_j)]$$

1st-Order Quadrupolar (a few MHz)

$$\Omega_q^{(1)} = \omega_q [\mathbb{D}^{\{q\}}(\Theta) \cdot \mathbb{d}_I(m_i, m_j)]$$

2nd-Order Quadrupolar (a few kHz)

$$\Omega_q^{(2)} = \frac{\omega_q^2}{\omega_0} [\mathbb{S}^{\{qq\}} \cdot \mathbb{C}_0(m_i, m_j)] + \frac{\omega_q^2}{\omega_0} [\mathbb{D}^{\{qq\}}(\Theta) \cdot \mathbb{C}_2(m_i, m_j)] + \frac{\omega_q^2}{\omega_0} [\mathbb{G}^{\{qq\}}(\Theta) \cdot \mathbb{C}_4(m_i, m_j)]$$

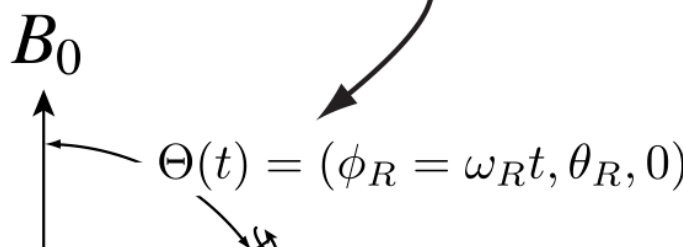
All **Isotropic contributions** contain the **S** spatial function.

Need to eliminate all **anisotropic contributions** to get high resolution spectra

- Only excite m to -m transitions, so $\mathbb{d}_I(m, -m) = 0$

Sample Rotation & Spatial Symmetry Pathways

Spatial Pathway

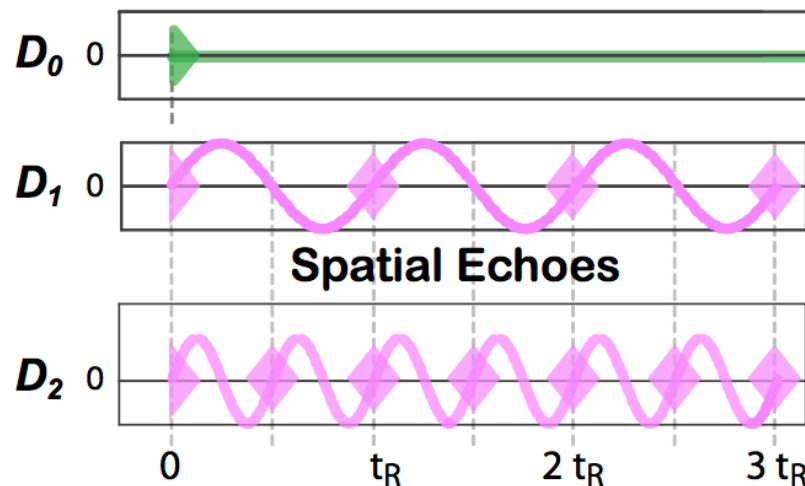
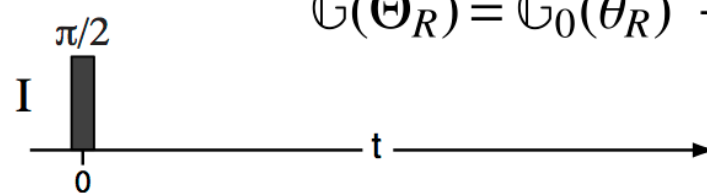


$$\mathbb{P}(\Theta_R) = \mathbb{P}_0(\theta_R) + \mathbb{P}_1(\theta_R, \phi_R)$$

$$\mathbb{D}(\Theta_R) = \mathbb{D}_0(\theta_R) + \mathbb{D}_1(\theta_R, \phi_R) + \mathbb{D}_2(\theta_R, \phi_R)$$

$$\mathbb{F}(\Theta_R) = \mathbb{F}_0(\theta_R) + \mathbb{F}_1(\theta_R, \phi_R) + \mathbb{F}_2(\theta_R, \phi_R) + \mathbb{F}_3(\theta_R, \phi_R)$$

$$\mathbb{G}(\Theta_R) = \mathbb{G}_0(\theta_R) + \mathbb{G}_1(\theta_R, \phi_R) + \mathbb{G}_2(\theta_R, \phi_R) + \mathbb{G}_3(\theta_R, \phi_R) + \mathbb{G}_4(\theta_R, \phi_R)$$



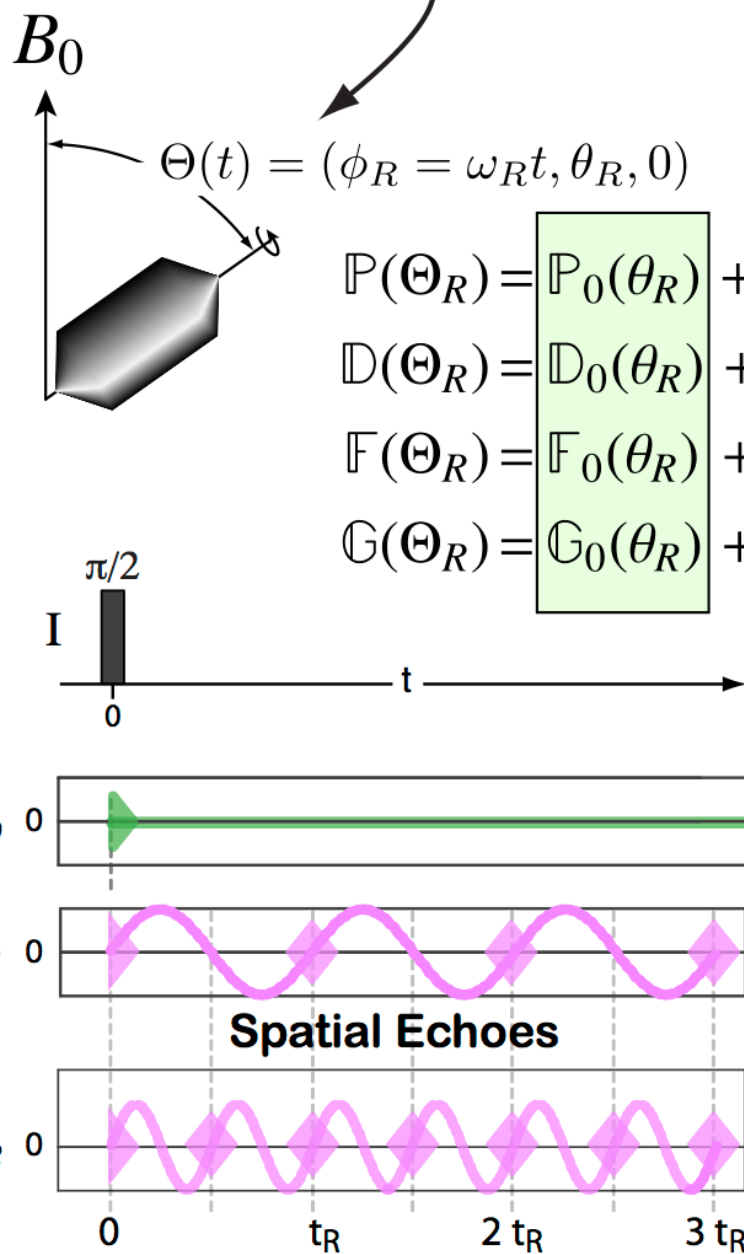
During sample motion S is invariant, and other spatial parts break up into

Roots of $\mathcal{P}_L(\cos \theta)$, where n=0 spatial components are zero

L	$\theta_M^{(L)}$	Method
\mathbb{P}_0	90.00°	P-MAS
\mathbb{D}_0	54.74°	D-MAS
\mathbb{F}_0	39.23°	F-MAS
\mathbb{G}_0	30.56°	G-MAS
	90.00°	
	70.12°	

Sample Rotation & Spatial Symmetry Pathways

Spatial Pathway



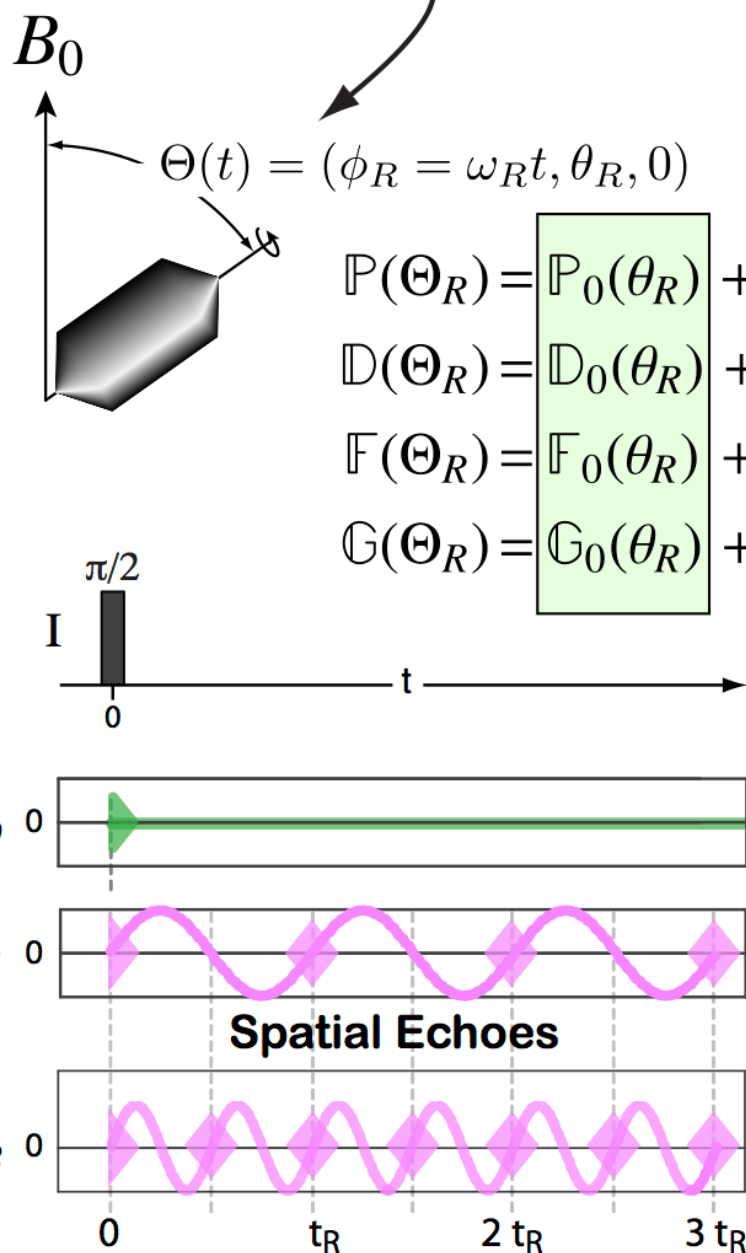
During sample motion S is invariant, and other spatial parts break up into

Roots of $\mathcal{P}_L(\cos \theta)$, where n=0 spatial components are zero

L	$\theta_M^{(L)}$	Method
\mathbb{P}_0	90.00°	P-MAS
\mathbb{D}_0	54.74°	D-MAS
\mathbb{F}_0	39.23°	F-MAS
\mathbb{G}_0	30.56°	G-MAS
	90.00°	
	70.12°	

Sample Rotation & Spatial Symmetry Pathways

Spatial Pathway



During sample motion S is invariant, and other spatial parts break up into

These cause spinning sidebands that go away at sufficiently high spinning speeds

Roots of $\mathcal{P}_L(\cos \theta)$, where n=0 spatial components are zero

L	$\theta_M^{(L)}$	Method
\mathbb{P}_0	90.00°	P-MAS
\mathbb{D}_0	54.74°	D-MAS
\mathbb{F}_0	39.23°	F-MAS
\mathbb{G}_0	30.56°	G-MAS
	90.00°	
	70.12°	

- Fast sample rotation at 54.74° eliminates **D** but not **G** spatial anisotropy

1st-Order Nuclear Shielding (a few kHz)

$$\Omega_{\sigma}^{(1)} = -\omega_0 \sigma_{iso} [\mathbb{S}^{\{\sigma\}} \cdot \mathbb{p}_I(m_i, m_j)] - \omega_0 \zeta_{\sigma} [\mathbb{D}_0^{\{\sigma\}}(\theta_R) \cdot \mathbb{p}_I(m_i, m_j)]$$

1st-Order Quadrupolar (a few MHz)

$$\Omega_q^{(1)} = \omega_q [\mathbb{D}^{\{q\}}(\Theta) \cdot \mathbb{d}_I(m_i, m_j)]$$

2nd-Order Quadrupolar (a few kHz)

$$\Omega_q^{(2)} = \frac{\omega_q^2}{\omega_0} [\mathbb{S}^{\{qq\}} \cdot \mathbb{C}_0(m_i, m_j)] + \frac{\omega_q^2}{\omega_0} [\mathbb{D}_0^{\{qq\}}(\theta_R) \cdot \mathbb{C}_2(m_i, m_j)] + \frac{\omega_q^2}{\omega_0} [\mathbb{G}_0^{\{qq\}}(\theta_R) \cdot \mathbb{C}_4(m_i, m_j)]$$

All **Isotropic contributions** contain the **S** spatial function.

Need to eliminate all **anisotropic contributions** to get high resolution spectra

- Only excite m to -m transitions, so $\mathbb{d}_I(m, -m) = 0$
- Fast sample rotation at 54.74° eliminates **D** but not **G** spatial anisotropy

- Fast sample rotation at 30.56° eliminates **G** but not **D** spatial anisotropy

1st-Order Nuclear Shielding (a few kHz)

$$\Omega_{\sigma}^{(1)} = -\omega_0 \sigma_{iso} [\mathbb{S}^{\{\sigma\}} \cdot \mathbb{p}_I(m_i, m_j)] - \omega_0 \zeta_{\sigma} [\mathbb{D}_0^{\{\sigma\}}(\theta_R) \cdot \mathbb{p}_I(m_i, m_j)]$$

1st-Order Quadrupolar (a few MHz)

$$\Omega_q^{(1)} = \omega_q [\mathbb{D}^{\{q\}}(\Theta) \cdot \mathbb{d}_I(m_i, m_j)]$$

2nd-Order Quadrupolar (a few kHz)

$$\Omega_q^{(2)} = \frac{\omega_q^2}{\omega_0} [\mathbb{S}^{\{qq\}} \cdot \mathbb{C}_0(m_i, m_j)] + \frac{\omega_q^2}{\omega_0} [\mathbb{D}_0^{\{qq\}}(\theta_R) \cdot \mathbb{C}_2(m_i, m_j)] + \frac{\omega_q^2}{\omega_0} [\mathbb{G}_0^{\{qq\}}(\theta_R) \cdot \mathbb{C}_4(m_i, m_j)]$$

All **Isotropic contributions** contain the **S** spatial function.

Need to eliminate all **anisotropic contributions** to get high resolution spectra

- Only excite m to -m transitions, so $\mathbb{d}_I(m, -m) = 0$
- Fast sample rotation at 30.56° eliminates **G** but not **D** spatial anisotropy

Quadrupolar MAS Frequency Contributions

1st-Order Nuclear Shielding (a few kHz)

$$\Omega_{\sigma}^{(1)} = -\omega_0 \sigma_{iso} [S^{\{\sigma\}} \cdot p_I(m_i, m_j)] - \omega_0 \zeta_{\sigma} [D_0^{\{\sigma\}}(\theta) \cdot c_I(m_i, m_j)]$$

1st-Order Quadrupolar (a few MHz)

$$\Omega_q^{(1)} = \omega_q [D^{\{q\}}(\Theta) \cdot d_I(m_i, m_j)]$$

2nd-Order Quadrupolar (few kHz)

$$\Omega_q^{(2)} = \frac{\omega_q^2}{\omega_0} [S^{\{q\}}(\theta_0, m_i, m_j) + \frac{\omega_q^2}{\omega_0} [D^{\{q\}}(\theta_R) \cdot c_2(m_i, m_j)] + \frac{\omega_q^2}{\omega_0} [G^{\{qq\}}(\theta_R) \cdot c_4(m_i, m_j)]]$$

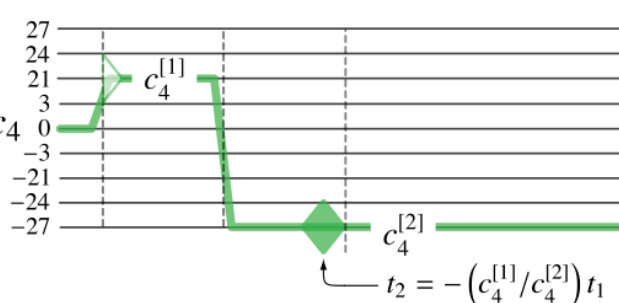
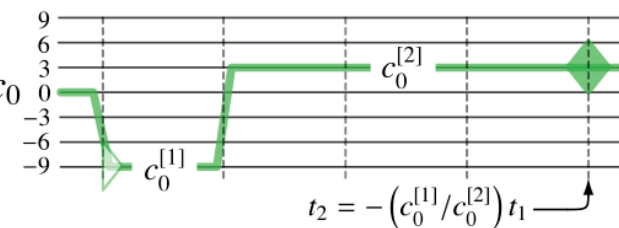
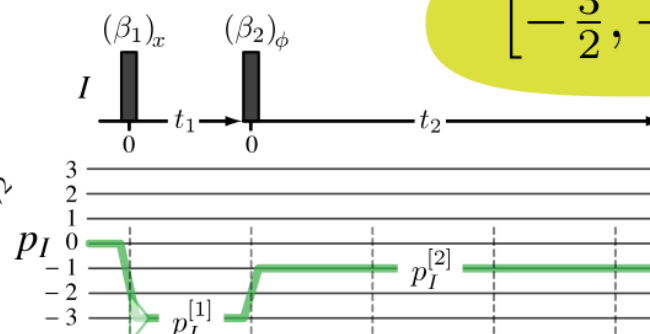
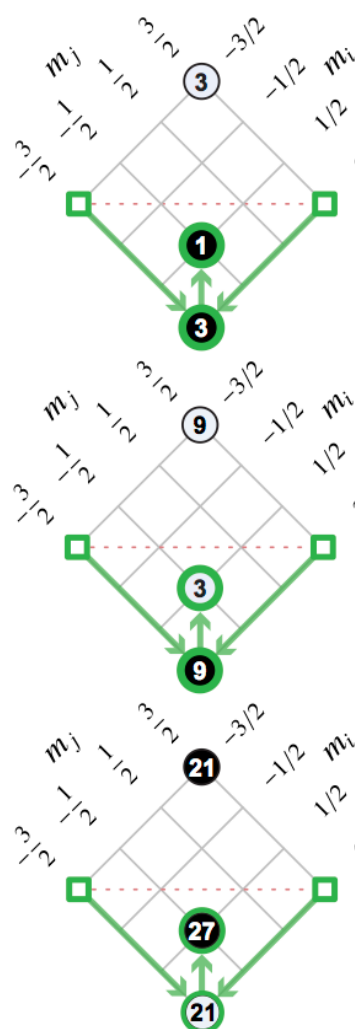
- Cannot be eliminated about any single rotor angle axis**
- | L | $\theta_M^{(L)}$ | Method |
|----------------|------------------|--------|
| P ₀ | 90.00° | P-MAS |
| D ₀ | 54.74° | D-MAS |
| F ₀ | 39.23° | F-MAS |
| G ₀ | 30.56° | G-MAS |
- Fast sample rotation at 54.74° eliminates D but not G spatial anisotropy
 - Fast sample rotation at 30.56° eliminates G but not D spatial anisotropy

How to get high resolution spectra of Quadrupolar Nuclei

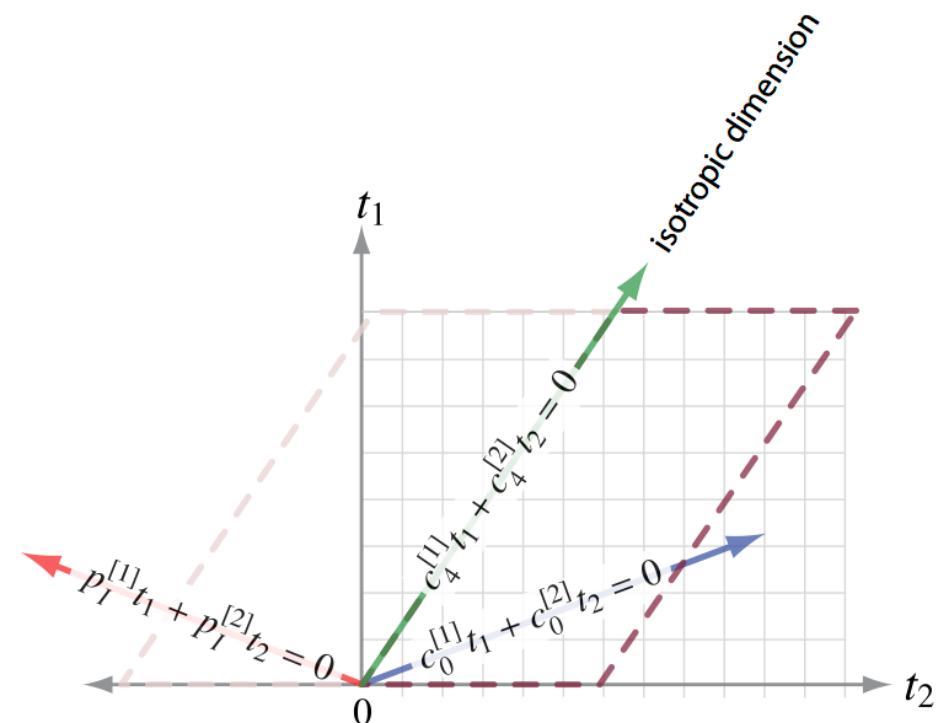
with a little help from
symmetry pathways

MQ-MAS uses a c₄ echo to refocus residual anisotropy

$$\langle \Omega \rangle_{\text{MAS}} = -\omega_0 \sigma_{iso} [\mathbb{S}^{\{\sigma\}} \cdot \mathbb{p}_I(m_i, m_j)] + \frac{\omega_q^2}{\omega_0} [\mathbb{S}^{\{qq\}} \cdot \mathbb{c}_0(m_i, m_j)] + \frac{\omega_q^2}{\omega_0} [\mathbb{G}_0^{\{qq\}}(\theta_M^{(2)}) \cdot \mathbb{c}_4(m_i, m_j)]$$

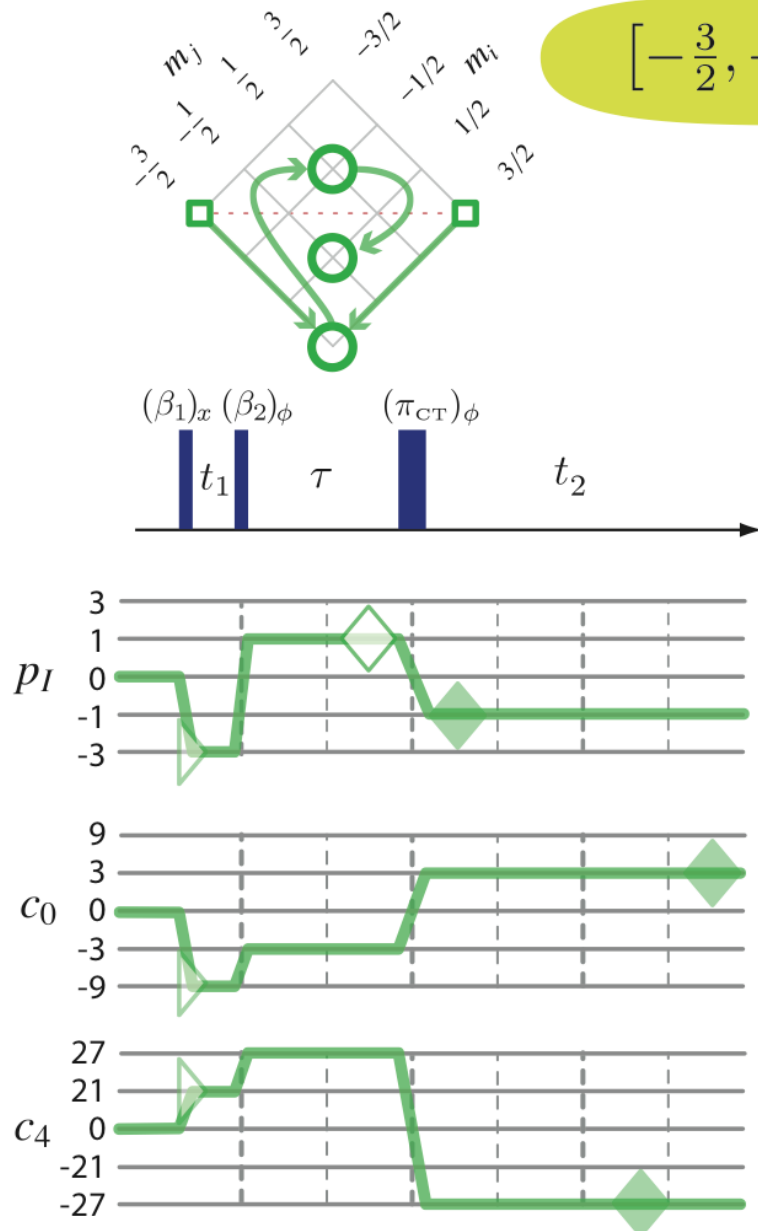


$$[-\frac{3}{2}, +\frac{3}{2}] \rightarrow \left| -\frac{3}{2} \right\rangle \left\langle +\frac{3}{2} \right|_{t_1} \rightarrow \left| -\frac{1}{2} \right\rangle \left\langle +\frac{1}{2} \right|_{t_2}$$



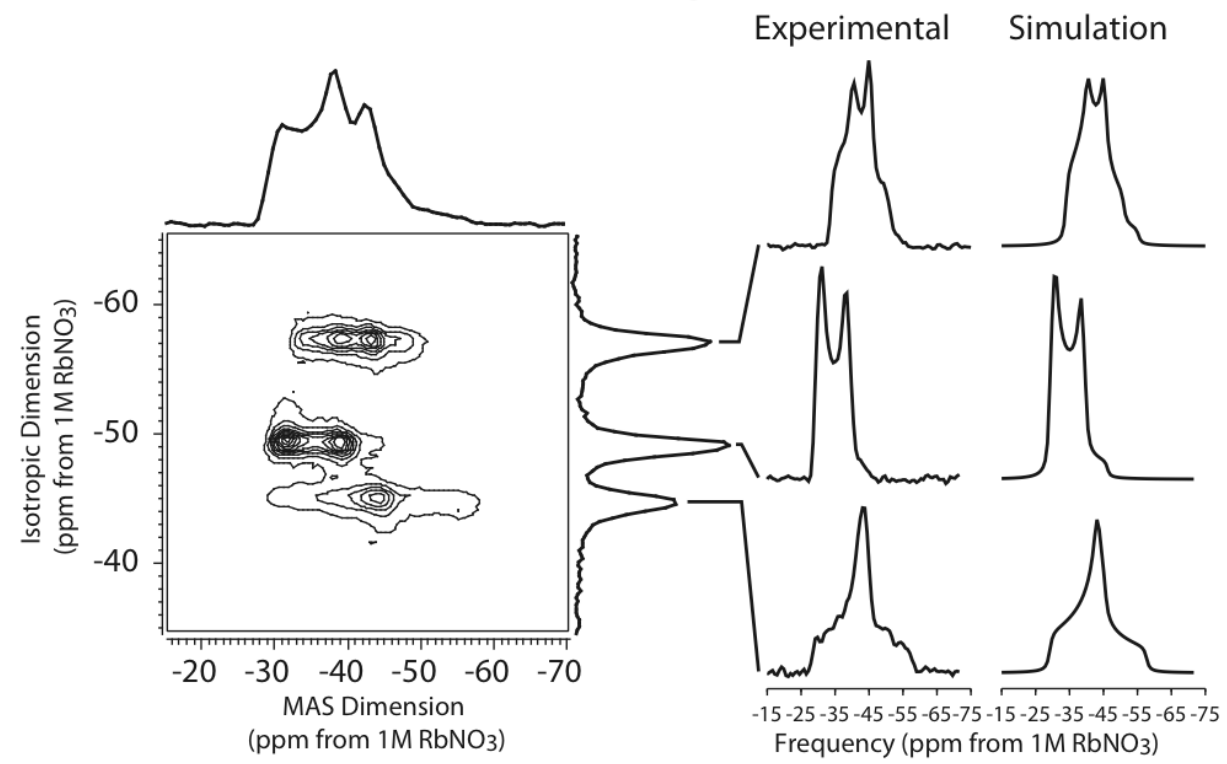
Frydman and Harwood,
J. Am. Chem. Soc., 117, 5367 (1995)
 Medek, Harwood, and Frydman,
J. Am. Chem. Soc., 117, 12779 (1995)

2D Shifted-Echo 3Q-MAS



$$\left[-\frac{3}{2}, +\frac{3}{2} \right] \rightarrow \left| -\frac{3}{2} \right\rangle \left\langle +\frac{3}{2} \right|_{t_1} \rightarrow \left| \frac{1}{2} \right\rangle \left\langle -\frac{1}{2} \right|_{\tau} \rightarrow \left| -\frac{1}{2} \right\rangle \left\langle +\frac{1}{2} \right|_{t_2}$$

^{87}Rb MQ-MAS Spectrum of RbNO_3
After Shearing Transformation



Massiot et al., *SSNMR*, **6**, 73 (1996)

MQ-MAS c₄ echo transition pathway possibilities increase with spin

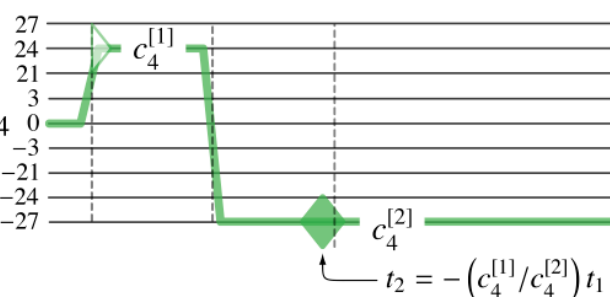
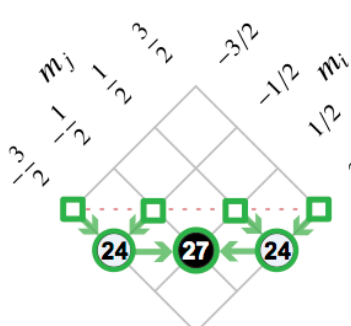
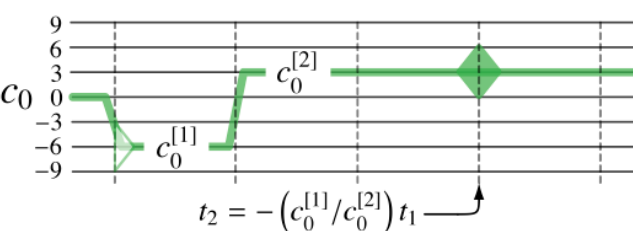
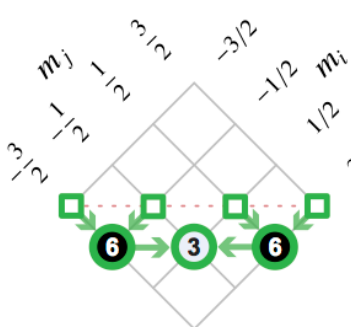
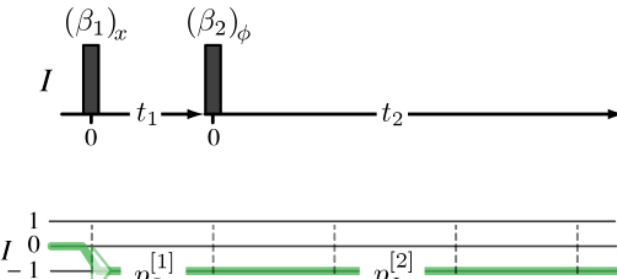
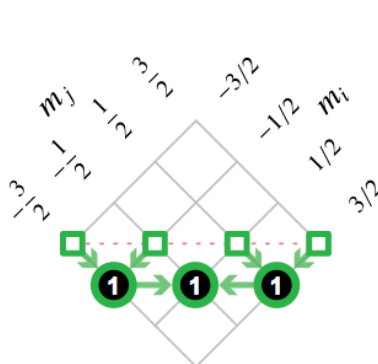
$$\langle \Omega \rangle_{\text{MAS}} = -\omega_0 \sigma_{iso} [\mathbb{S}^{\{\sigma\}} \cdot \mathbb{p}_I(m_i, m_j)] + \frac{\omega_q^2}{\omega_0} [\mathbb{S}^{\{qq\}} \cdot \mathbb{C}_0(m_i, m_j)] + \frac{\omega_q^2}{\omega_0} [\mathbb{G}_0^{\{qq\}}(\theta_M^{(2)}) \cdot \mathbb{C}_4(m_i, m_j)]$$

Transition $ m_j\rangle\langle m_i $	$I = 9/2$ $p_I \quad c_0 \quad c_4$		
$\left \frac{9}{2} \right\rangle \left\langle -\frac{9}{2} \right $	$I = 7/2$ $p_I \quad c_0 \quad c_4$		
$\left \frac{7}{2} \right\rangle \left\langle -\frac{7}{2} \right $	$I = 5/2$ $p_I \quad c_0 \quad c_4$		
$\left \frac{5}{2} \right\rangle \left\langle -\frac{5}{2} \right $ $p_I \quad c_0 \quad c_4$	$I = 3/2$ $p_I \quad c_0 \quad c_4$	$I = 5/2$ $p_I \quad c_0 \quad c_4$	$I = 9/2$ $p_I \quad c_0 \quad c_4$
$\left \frac{3}{2} \right\rangle \left\langle -\frac{3}{2} \right $	3 9 21	3 6 114	7 147 483
$\left \frac{1}{2} \right\rangle \left\langle -\frac{1}{2} \right $	1 3 27	1 8 72	1 15 135
Central Transition $\left -\frac{1}{2} \right\rangle \left\langle \frac{1}{2} \right $	1 3 27	1 8 72	1 15 135
$\left -\frac{3}{2} \right\rangle \left\langle \frac{3}{2} \right $	3 9 21	3 6 114	3 27 303
$\left -\frac{5}{2} \right\rangle \left\langle \frac{5}{2} \right $		5 50 150	5 15 165
$\left -\frac{7}{2} \right\rangle \left\langle \frac{7}{2} \right $			7 147 483
$\left -\frac{9}{2} \right\rangle \left\langle \frac{9}{2} \right $			9 324 1116

Values inside solid black circles are negative

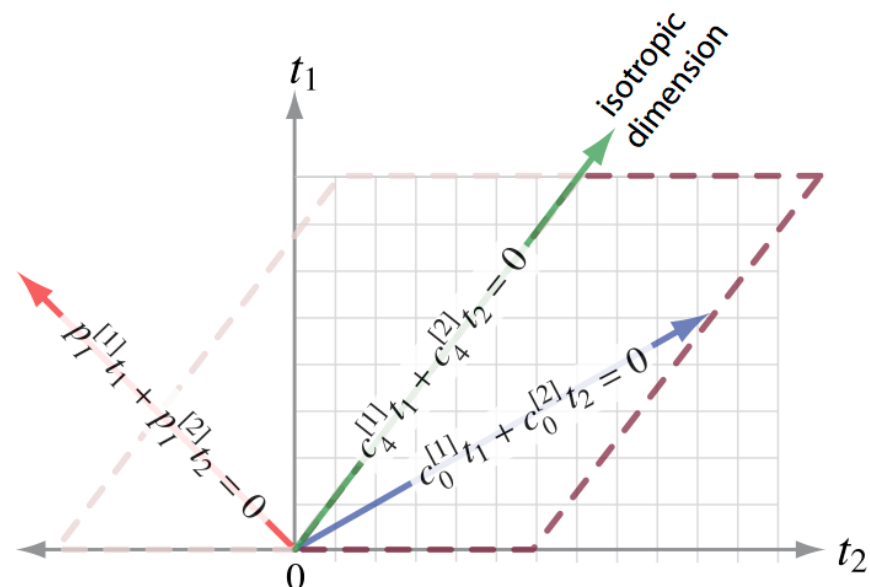
ST-MAS also uses a c₄ echo to refocus residual anisotropy

$$\langle \Omega \rangle_{\text{MAS}} = -\omega_0 \sigma_{iso} [\mathbb{S}^{\{\sigma\}} \cdot \mathbb{p}_I(m_i, m_j)] + \frac{\omega_q^2}{\omega_0} [\mathbb{S}^{\{qq\}} \cdot \mathbb{C}_0(m_i, m_j)] + \frac{\omega_q^2}{\omega_0} [\mathbb{G}_0^{\{qq\}}(\theta_M^{(2)}) \cdot \mathbb{C}_4(m_i, m_j)]$$



$$[-\frac{3}{2}, -\frac{1}{2}] \rightarrow |-\frac{3}{2}\rangle \langle -\frac{1}{2}|_{t_1} \rightarrow |-\frac{1}{2}\rangle \langle +\frac{1}{2}|_{t_2}$$

$$[\frac{1}{2}, \frac{3}{2}] \rightarrow |+\frac{1}{2}\rangle \langle +\frac{3}{2}|_{t_1} \rightarrow |-\frac{1}{2}\rangle \langle +\frac{1}{2}|_{t_2}$$



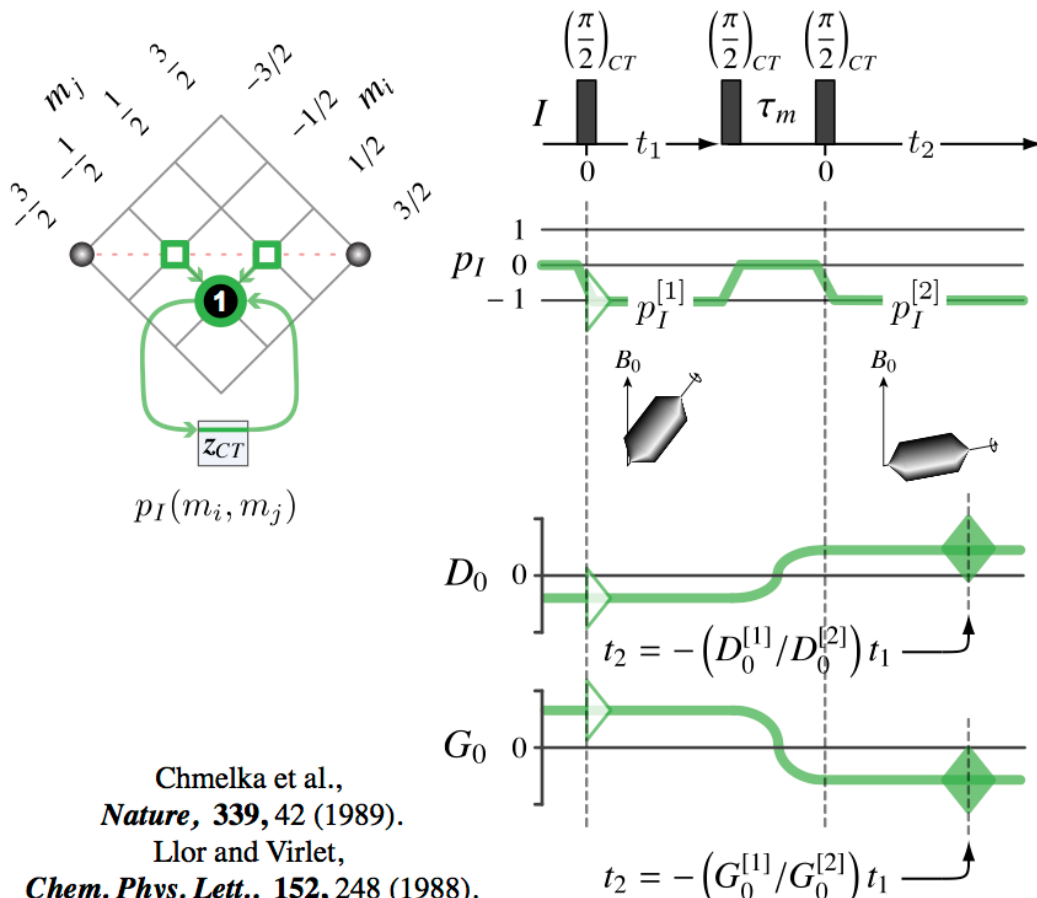
Requires extremely accurate setting of the magic angle.

Z. Gan, *J. Am. Chem. Soc.*, **122**, 3242-3243 (2000)

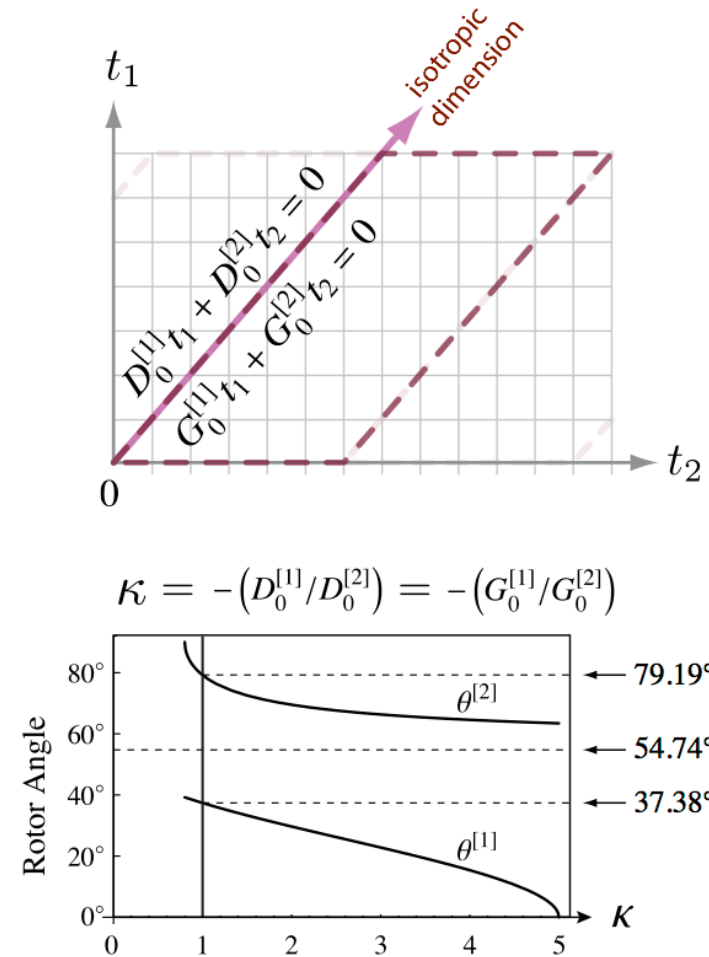
DAS uses simultaneous D₀ and G₀ echoes to refocus residual anisotropy

$$\left\langle \Omega^{\{\sigma\}} \right\rangle_{\text{VAS}} = -\omega_0 \sigma_{\text{iso}} [\mathbb{S}^{\{\sigma\}} \cdot \mathbb{p}_I(m_i, m_j)] - \omega_0 \zeta_{\sigma} [\mathbb{D}_0^{\{\sigma\}}(\theta_R) \cdot \mathbb{p}_I(m_i, m_j)]$$

$$\left\langle \Omega^{\{qq\}} \right\rangle_{\text{VAS}} = \frac{\omega_q^2}{\omega_0} [\mathbb{S}^{\{qq\}} \cdot \mathbb{C}_0(m_i, m_j)] + \frac{\omega_q^2}{\omega_0} [\mathbb{D}_0^{\{qq\}}(\theta_R) \cdot \mathbb{C}_2(m_i, m_j)] + \frac{\omega_q^2}{\omega_0} [\mathbb{G}_0^{\{qq\}}(\theta_R) \cdot \mathbb{C}_4(m_i, m_j)]$$

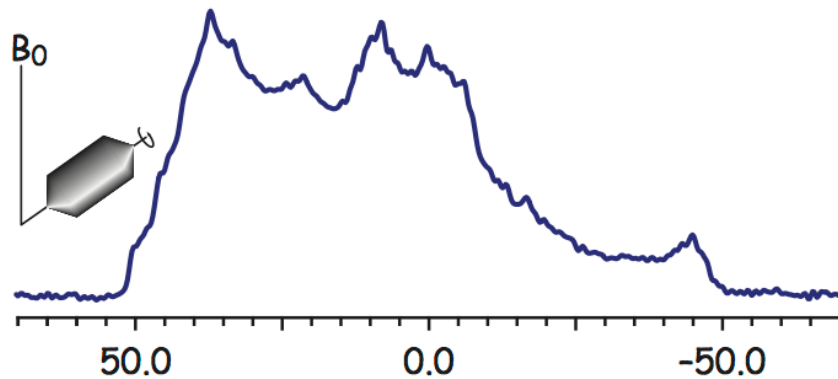


Need probe that can flip rotor angle during experiment.

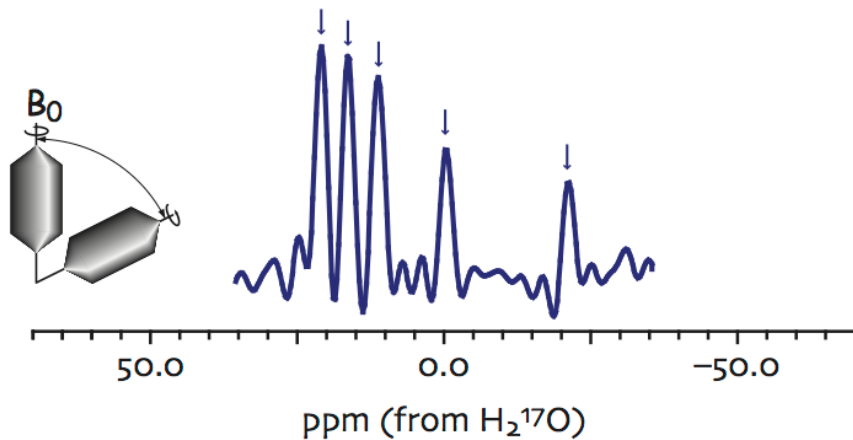


^{17}O 2D DAS of Coesite (A SiO_2 Crystalline Polymorph)

MAGIC-ANGLE SPINNING

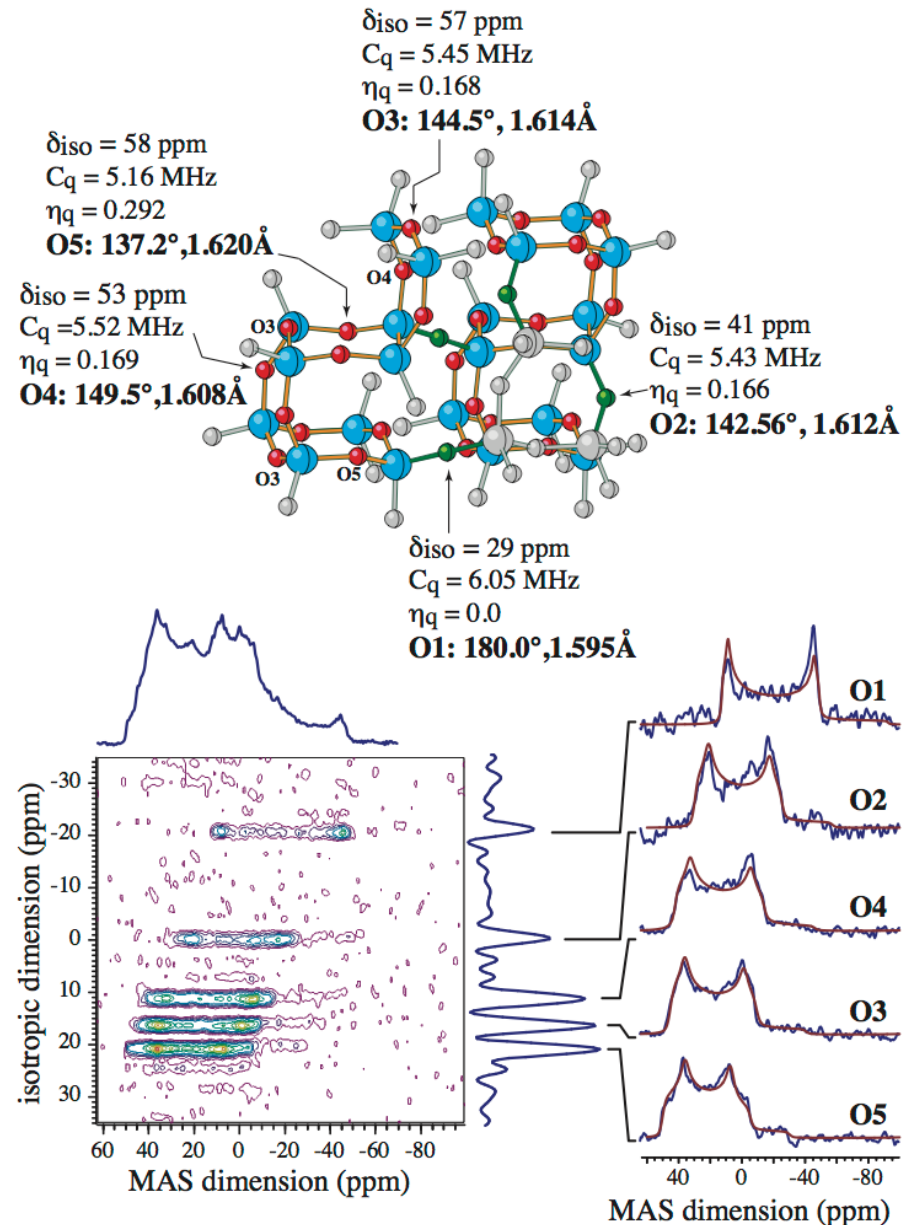


DYNAMIC-ANGLE SPINNING



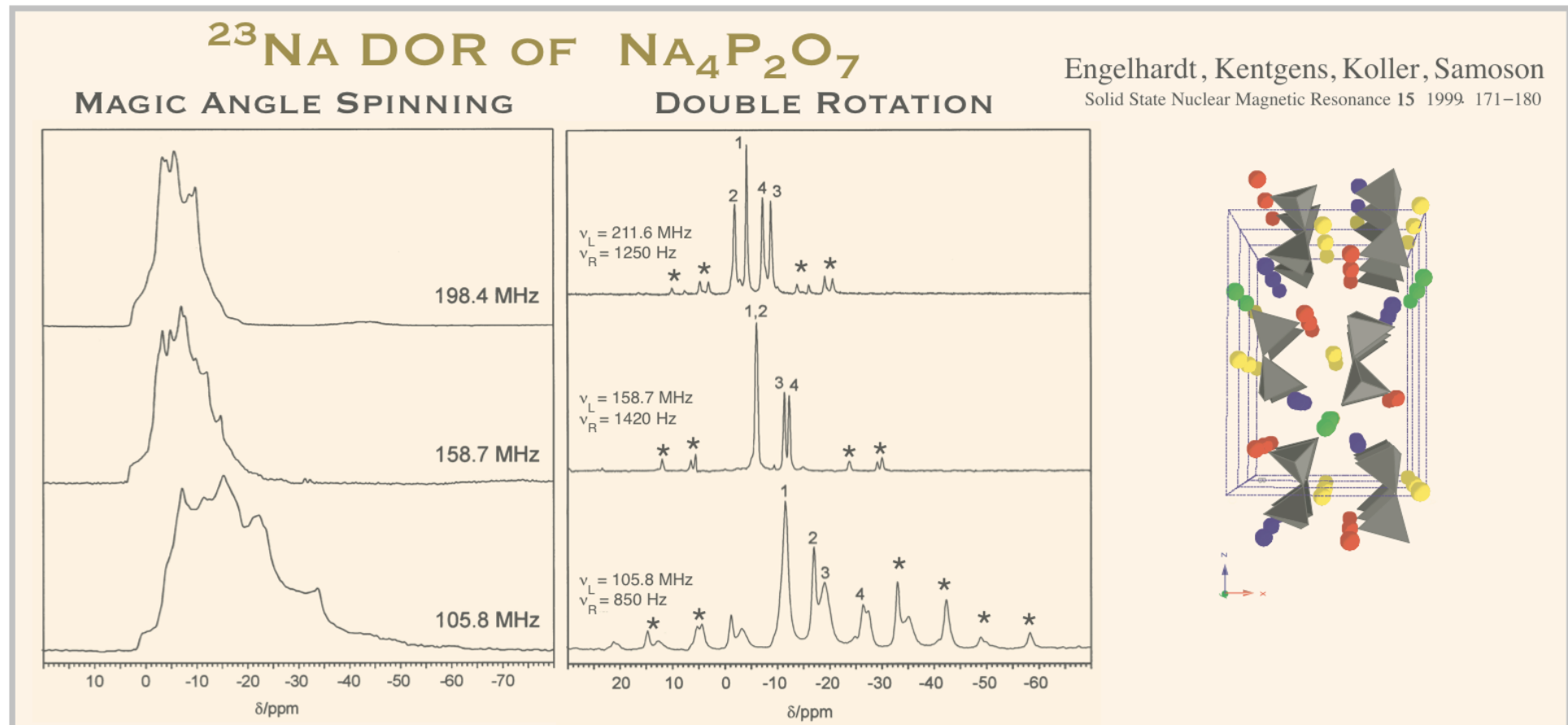
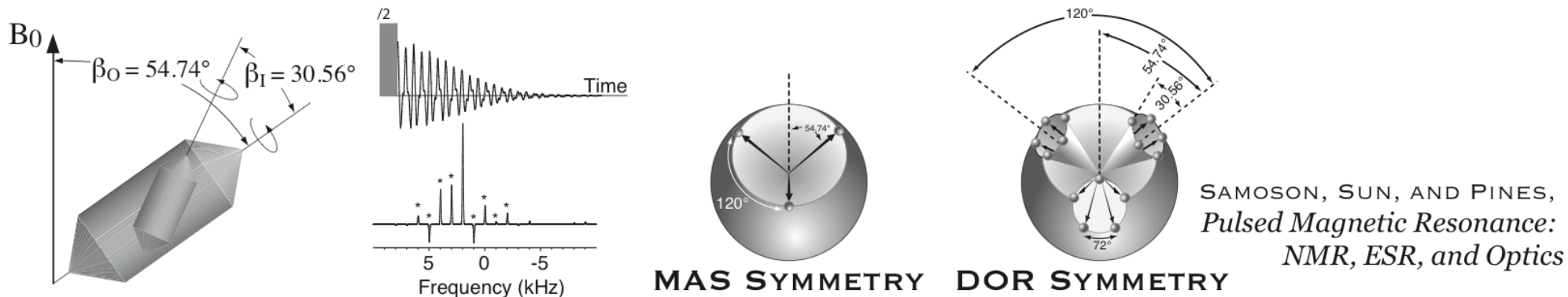
J. Phys. Chem., **99**, 12341 (1995)

COESITE STRUCTURAL FRAGMENT



A challenging Solution: Double Rotation

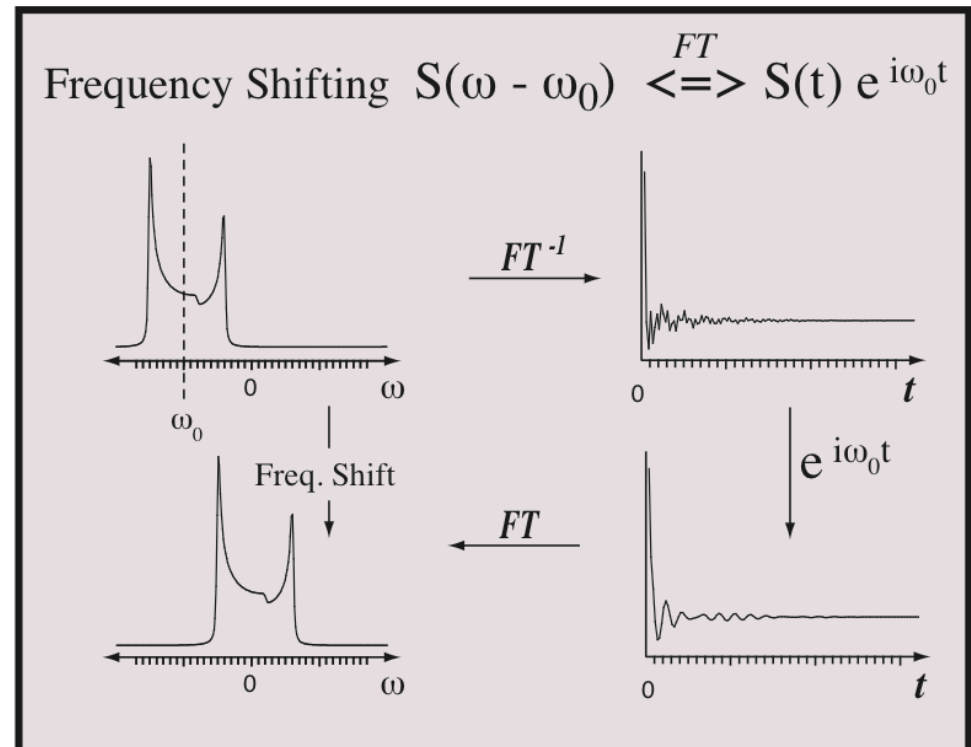
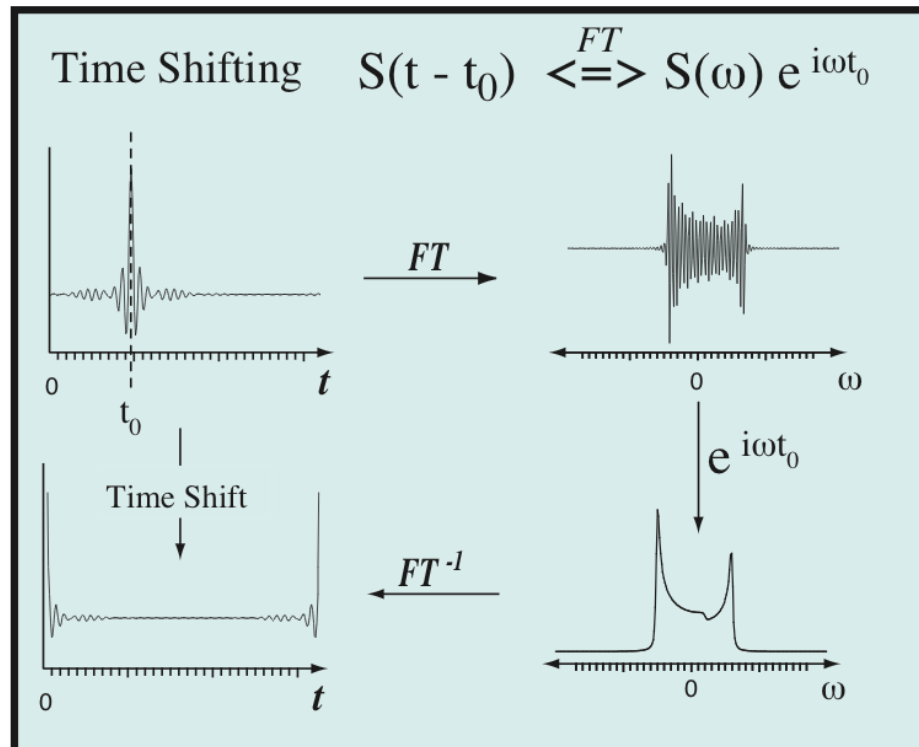
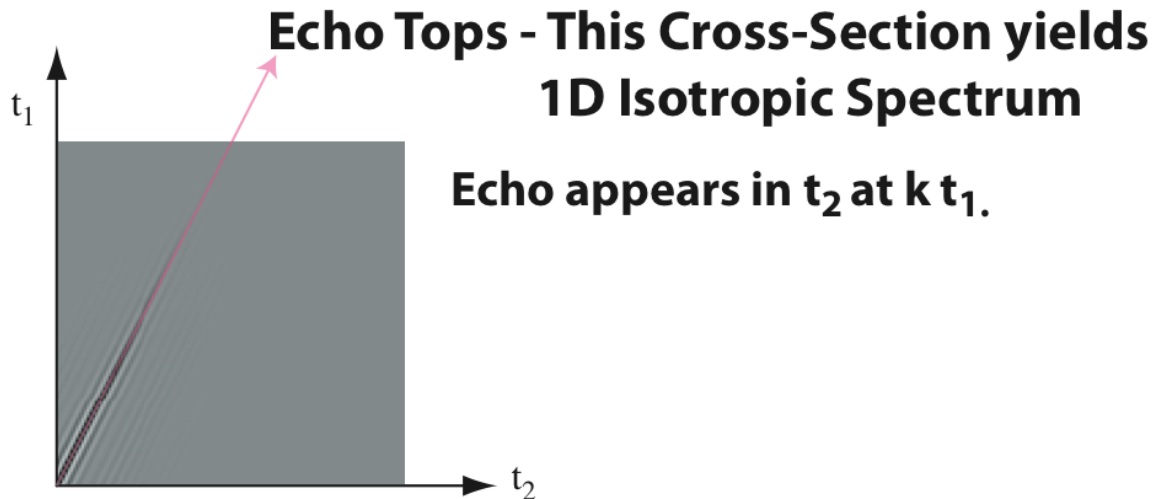
Samoson, Lippmaa, Pines, Mol. Phys., 65, 1023(1988).



Advantages		Disadvantages	
DOR	<ul style="list-style-type: none"> • Quantitative • High Sensitivity • Low rf power • One dimensional experiment <ul style="list-style-type: none"> - Quick experiment (In principle) 	<ul style="list-style-type: none"> • Special Probe Required • Stable spinning requires finesse • Slow spinning speeds <ul style="list-style-type: none"> - (large # of sidebands) • Large coil ... low rf power <ul style="list-style-type: none"> - poor decoupling. 	
DAS	<ul style="list-style-type: none"> • Quantitative • High Sensitivity, even with nuclei having large quad. couplings • Low rf power • works well for dilute quadrupolar nuclei 	<ul style="list-style-type: none"> • Special Probe Required • Fails in presence of strong homonuclear dipolar couplings • long hop times (30 ms) limits use to samples with long longitudinal relaxation (rare problem). 	
MQ-MAS	<ul style="list-style-type: none"> • Easiest to implement (no special probe) • Works well for Abundant nuclei • Works well for nuclei with short longitudinal relaxation 	<ul style="list-style-type: none"> • Not always quantitative • requires high rf power for excitation and mixing • Poor sensitivity for large Cq • Complex spinning sideband behavior 	
ST-MAS	<ul style="list-style-type: none"> • Easy to implement (no special probe) • excites only single quantum transitions • Works well for Abundant nuclei • Works well for nuclei with short longitudinal relaxation 	<ul style="list-style-type: none"> • Sensitive to magic-angle misset ($< 0.01^\circ$) • stable spinning speed required. • requires high rf power for satellite excitation. • Poor sensitivity for large Cq • Not always quantitative • Complex spinning sideband behavior • fails to remove 3rd and other higher-order effects • Fails when there's motional averaging of satellite lineshapes. 	

Signal Processing

The Fourier Transform, Shift Theorem, and Shearing Transformations



Affine Transformation in DAS, MQ-MAS, ST-MAS

"Symmetry Pathways in Solid-State NMR",
Prog. NMR Spect. **59**, 121-196 (2011)

$$\mathbf{t}' = \mathbf{A}\mathbf{t}, \quad \text{where} \quad s'(\mathbf{t}) = s(\mathbf{A}\mathbf{t})$$

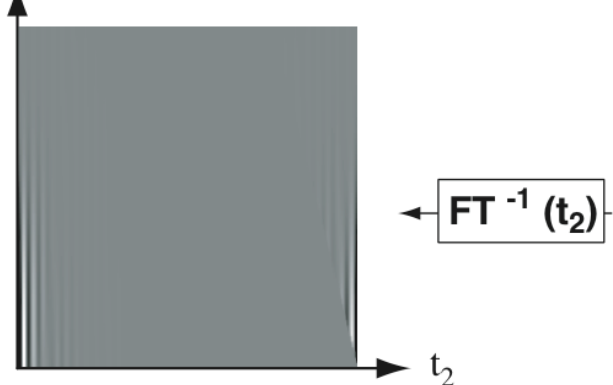
$$\mathbf{A} = \begin{pmatrix} 1+k & 0 \\ -k & 1 \end{pmatrix}$$

$$\tilde{\omega}' = \tilde{\omega}\mathbf{A}^{-1},$$

$$\text{where} \quad S'(\tilde{\omega}) = \frac{1}{|\mathbf{A}|}S(\tilde{\omega}\mathbf{A}^{-1})$$

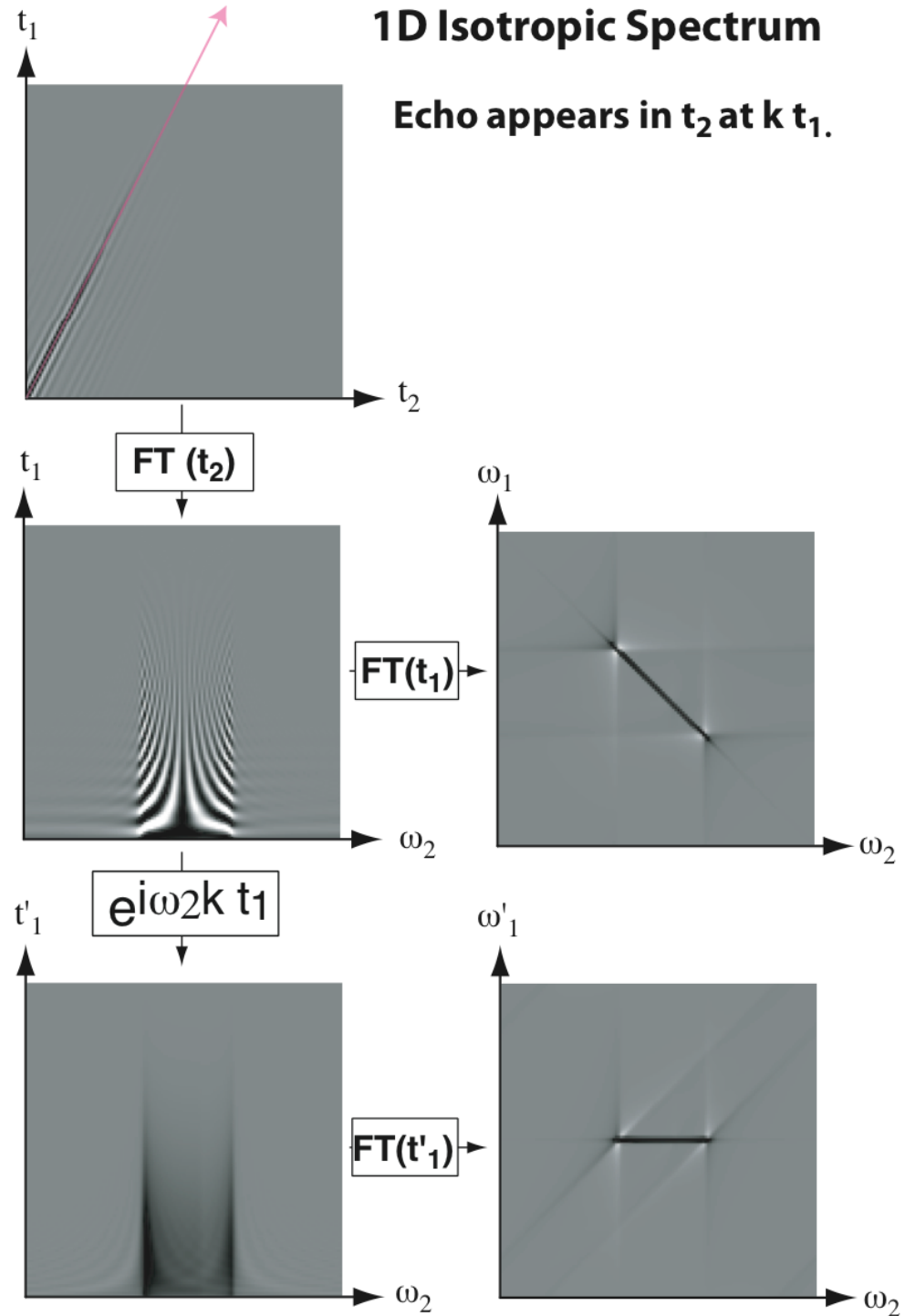
$$t'_1 = (1+k)t_1$$

$$t'_1 \quad \Delta t'_1 = (1+k)\Delta t_1$$

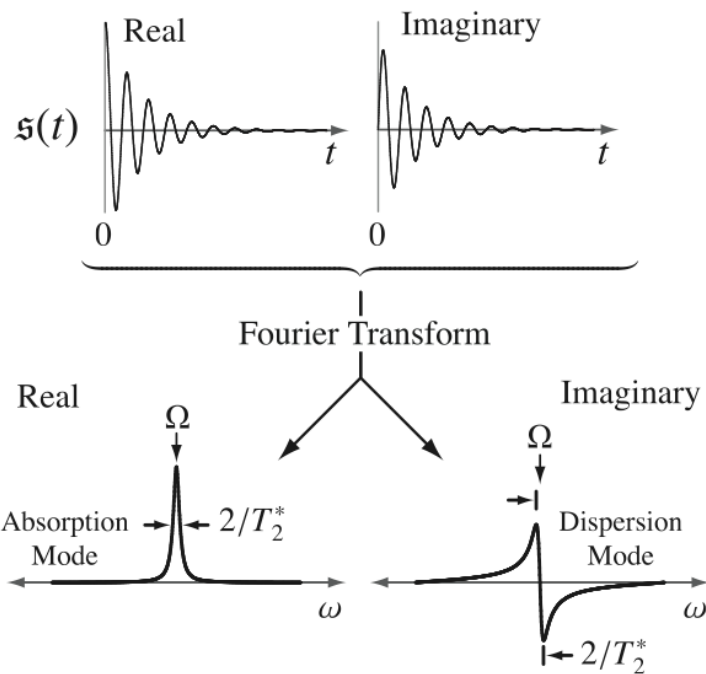


Echo Tops - This Cross-Section yields 1D Isotropic Spectrum

Echo appears in t_2 at $k t_1$.

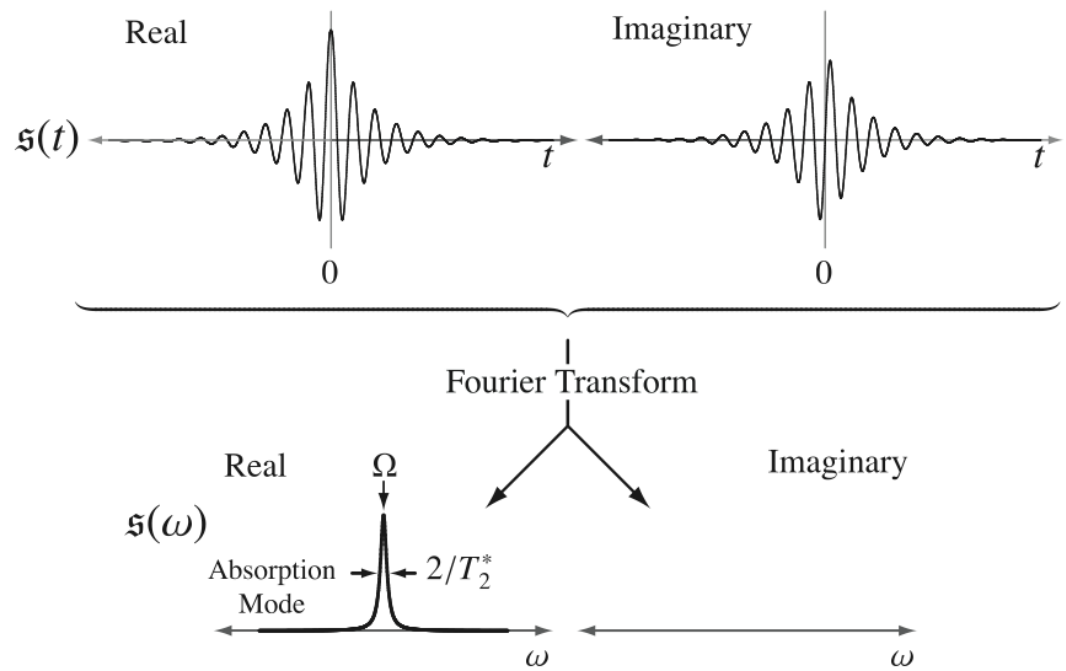


Absorption Mode Lineshapes One Dimension



$$s(\omega) = \int_0^\infty e^{-i\Omega t} e^{-|t|/T_2^*} e^{-i\omega t} dt$$

$$= \underbrace{\mathfrak{A}(\omega - \Omega)}_{\text{Real}} + i \underbrace{\mathfrak{D}(\omega - \Omega)}_{\text{Imaginary}}$$

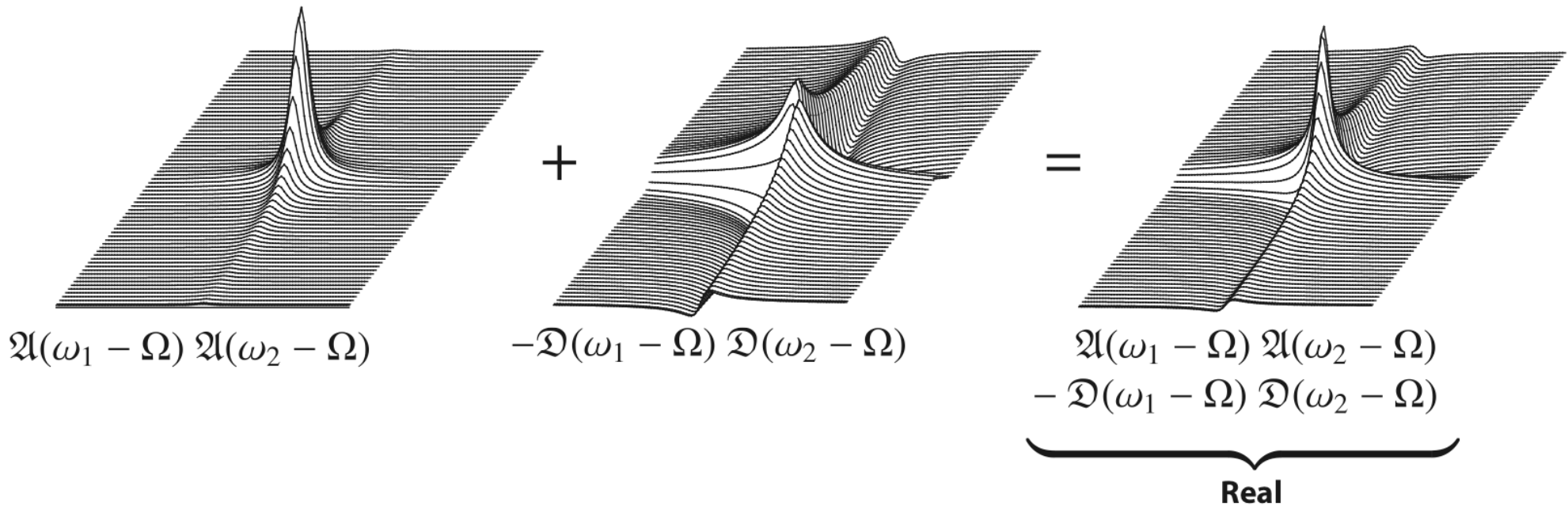


$$s(\omega) = \int_{-\infty}^\infty e^{-i\Omega t} e^{-|t|/T_2^*} e^{-i\omega t} dt$$

$$= \underbrace{2\mathfrak{A}(\omega - \Omega)}_{\text{Real}}$$

Absorption Mode Lineshapes Two Dimensions

$$\begin{aligned}\mathfrak{s}(\omega_1, \omega_2) &= \left[\int_0^\infty e^{-i\Omega t_1} e^{-|t_1|/T_2} e^{-i\omega_1 t_1} dt_1 \right] \times \left[\int_0^\infty e^{-i\Omega t_2} e^{-|t_2|/T_2} e^{-i\omega_2 t_2} dt_2 \right] \\ &= \underbrace{\mathfrak{A}(\omega_1 - \Omega) \mathfrak{A}(\omega_2 - \Omega) - \mathfrak{D}(\omega_1 - \Omega) \mathfrak{D}(\omega_2 - \Omega)}_{\text{Real}} + i \underbrace{[\mathfrak{A}(\omega_1 - \Omega) \mathfrak{D}(\omega_2 - \Omega) + \mathfrak{A}(\omega_2 - \Omega) \mathfrak{D}(\omega_1 - \Omega)]}_{\text{Imaginary}}\end{aligned}$$



Absorption Mode Lineshapes

Two Dimensions

Mathematical Solution: Just extend lower limits to negative infinity.

$$\begin{aligned}\mathfrak{s}(\omega_1, \omega_2) &= \left[\int_{-\infty}^{\infty} e^{-i\Omega t_1} e^{-|t_1|/T_2} e^{-i\omega_1 t_1} dt_1 \right] \times \left[\int_{-\infty}^{\infty} e^{-i\Omega t_2} e^{-|t_2|/T_2} e^{-i\omega_2 t_2} dt_2 \right] \\ &= \underbrace{4\mathfrak{A}(\omega_1 - \Omega)\mathfrak{A}(\omega_2 - \Omega)}_{\text{Real}}\end{aligned}$$

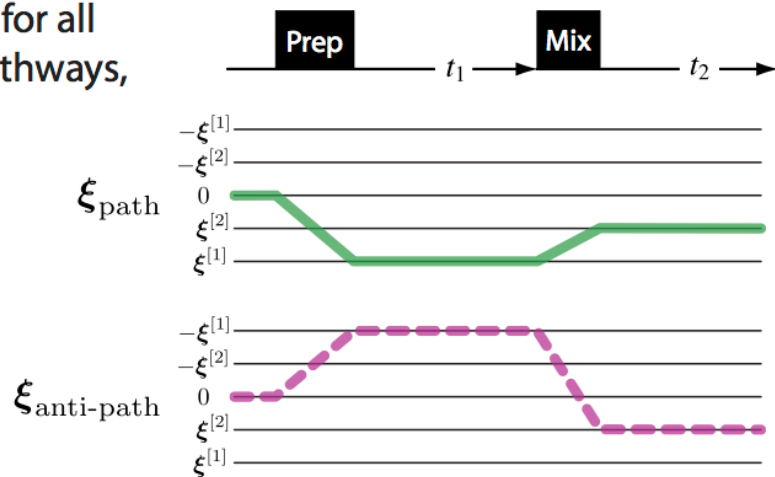
Actually, only need to extend one lower limit to negative infinity

$$\begin{aligned}\mathfrak{s}(\omega_1, \omega_2) &= \left[\int_{-\infty}^{\infty} e^{-i\Omega t_1} e^{-|t_1|/T_2} e^{-i\omega_1 t_1} dt_1 \right] \times \left[\int_0^{\infty} e^{-i\Omega t_2} e^{-|t_2|/T_2} e^{-i\omega_2 t_2} dt_2 \right] \\ &= \underbrace{2\mathfrak{A}(\omega_1 - \Omega)\mathfrak{A}(\omega_2 - \Omega)}_{\text{Real}} + \underbrace{i2\mathfrak{A}(\omega_1 - \Omega)\mathfrak{D}(\omega_1 - \Omega)}_{\text{Imaginary}}\end{aligned}$$

Absorption Mode Lineshapes Two Dimensions

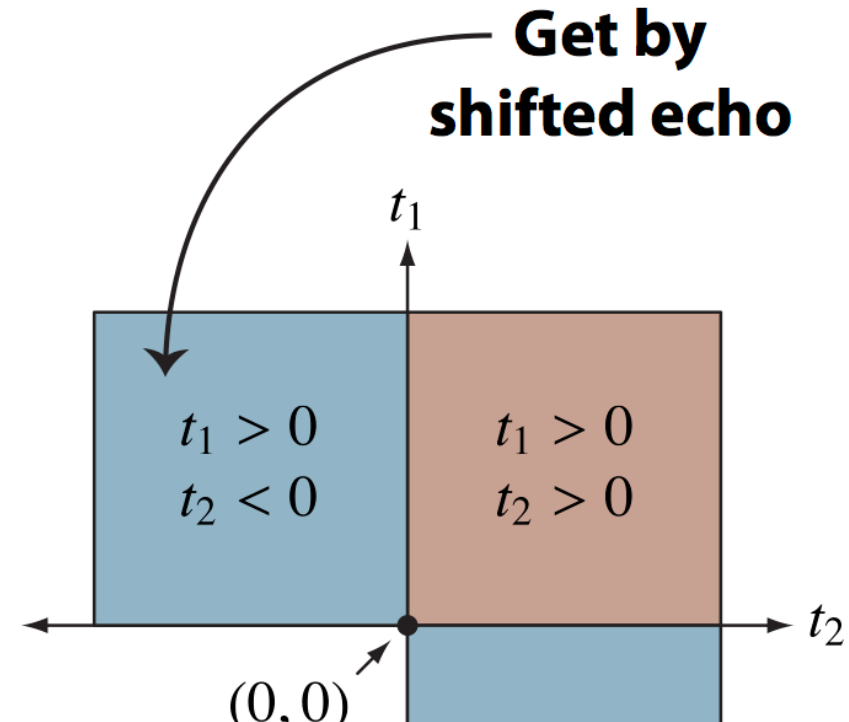
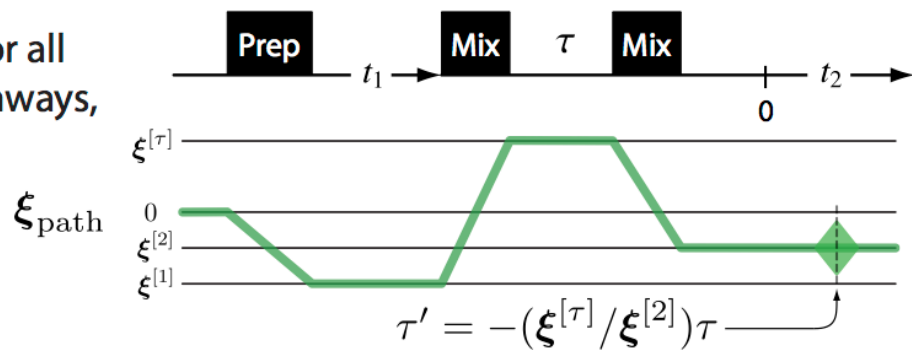
Hypercomplex Approach

Must be true for all symmetry pathways, not just \mathbf{p} .



Shifted Echo Approach

Must be true for all symmetry pathways, not just \mathbf{p} .

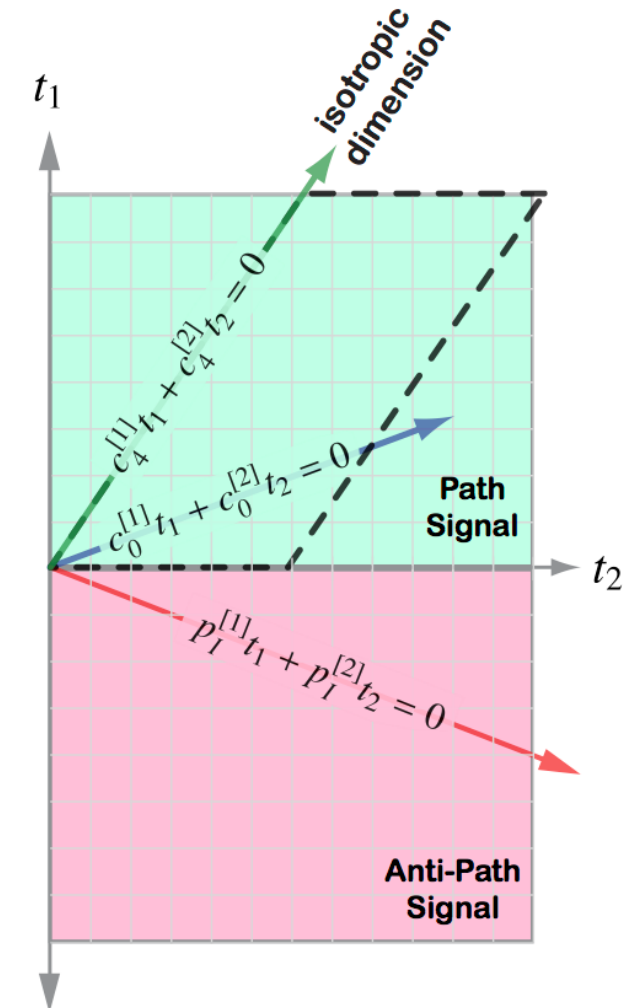
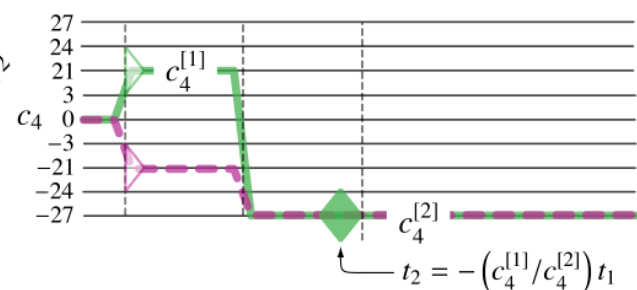
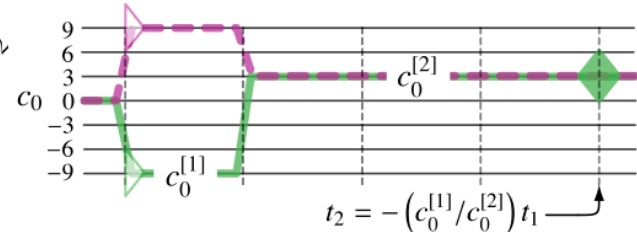
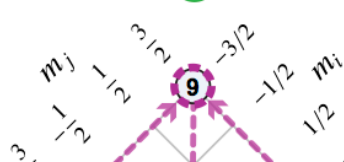
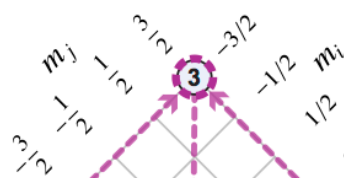


**Get by
shifted echo**

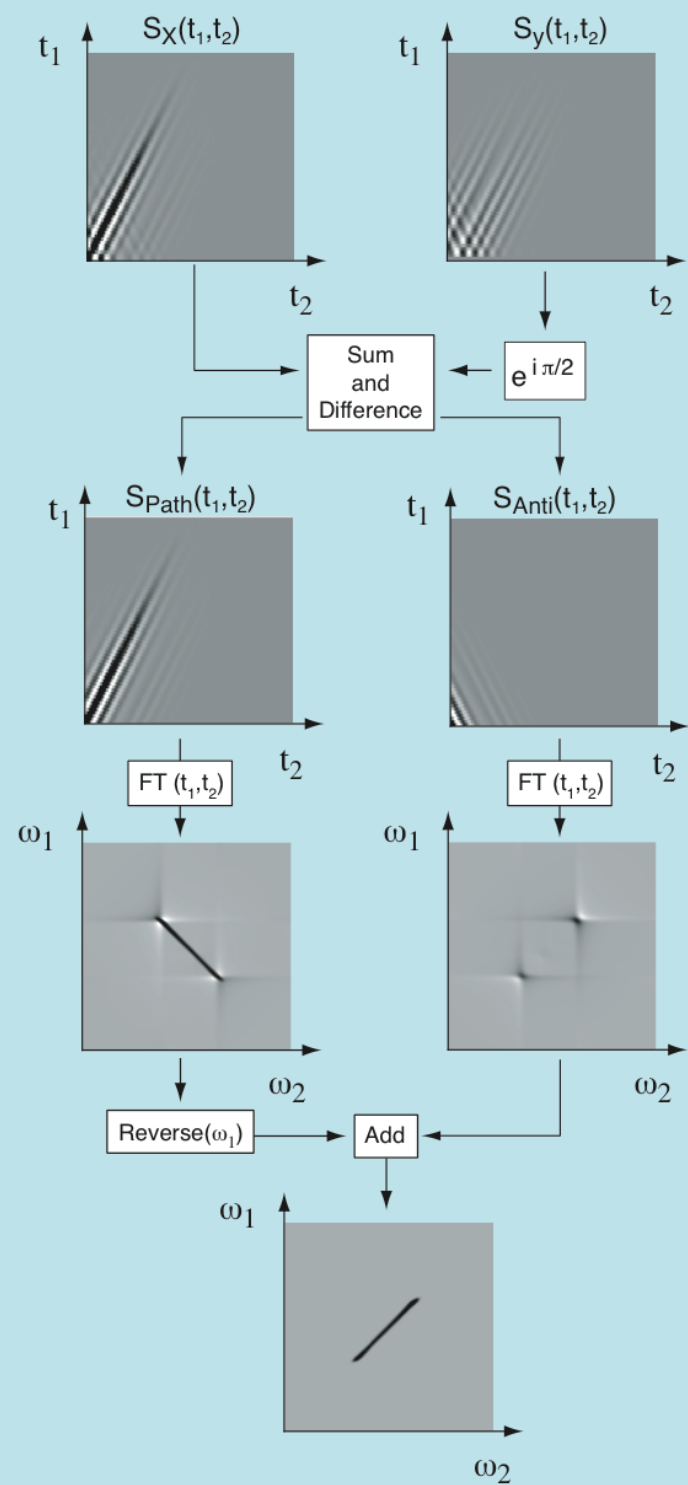
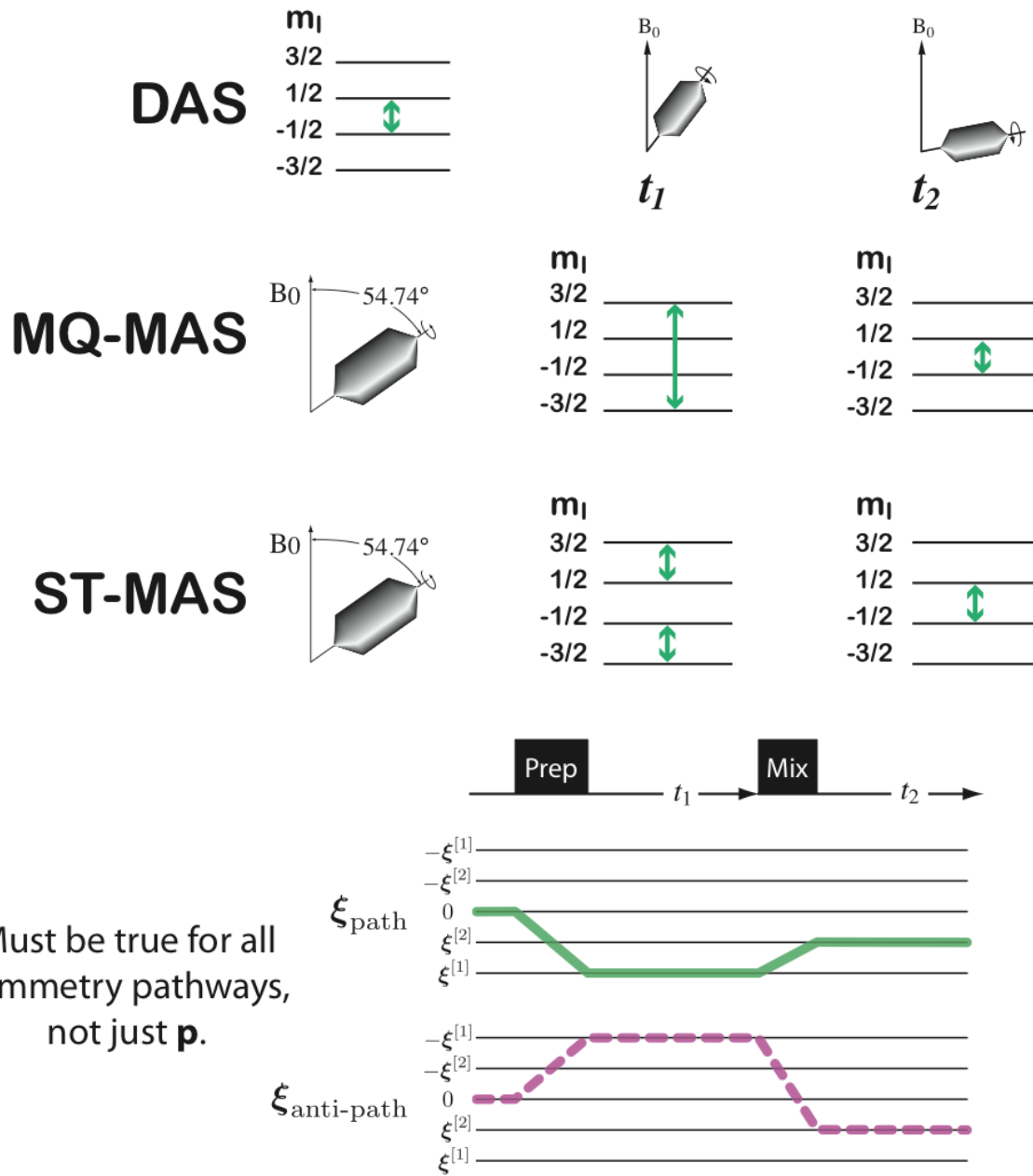
**Get by
hypercomplex**

MQ-MAS paths and antipaths

$$\langle \Omega \rangle_{\text{MAS}} = -\omega_0 \sigma_{iso} \left[S^{\{\sigma\}} \cdot p_I(m_i, m_j) \right] + \frac{\omega_q^2}{\omega_0} \left[S^{\{qq\}} \cdot c_0(m_i, m_j) \right] + \frac{\omega_q^2}{\omega_0} \left[G_0^{\{qq\}}(\theta_M^{(2)}) \cdot c_4(m_i, m_j) \right]$$

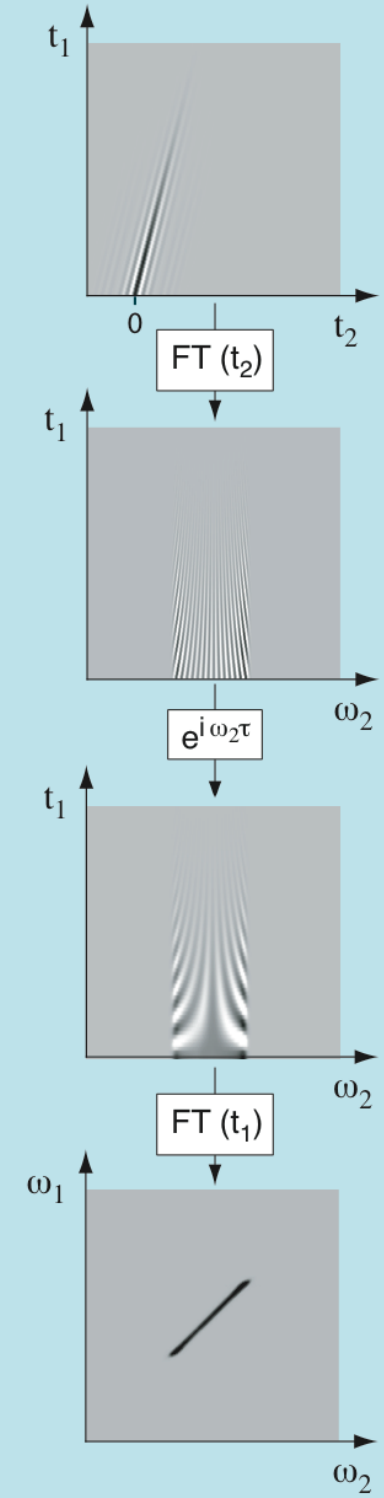
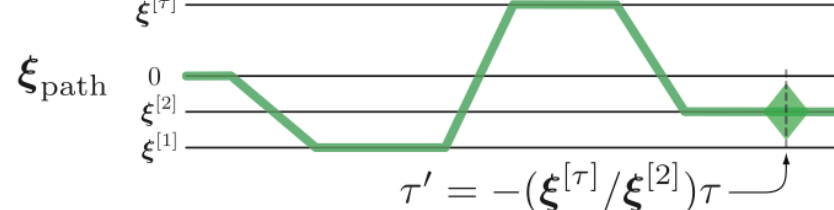
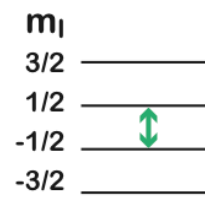
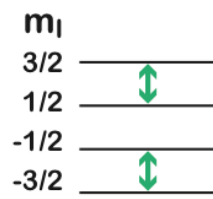
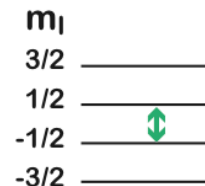
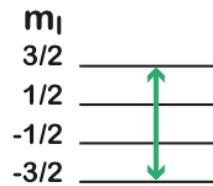
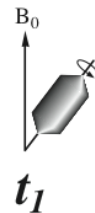
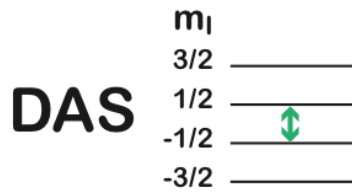


Hypercomplex Processing of DAS, MQ-MAS, ST-MAS



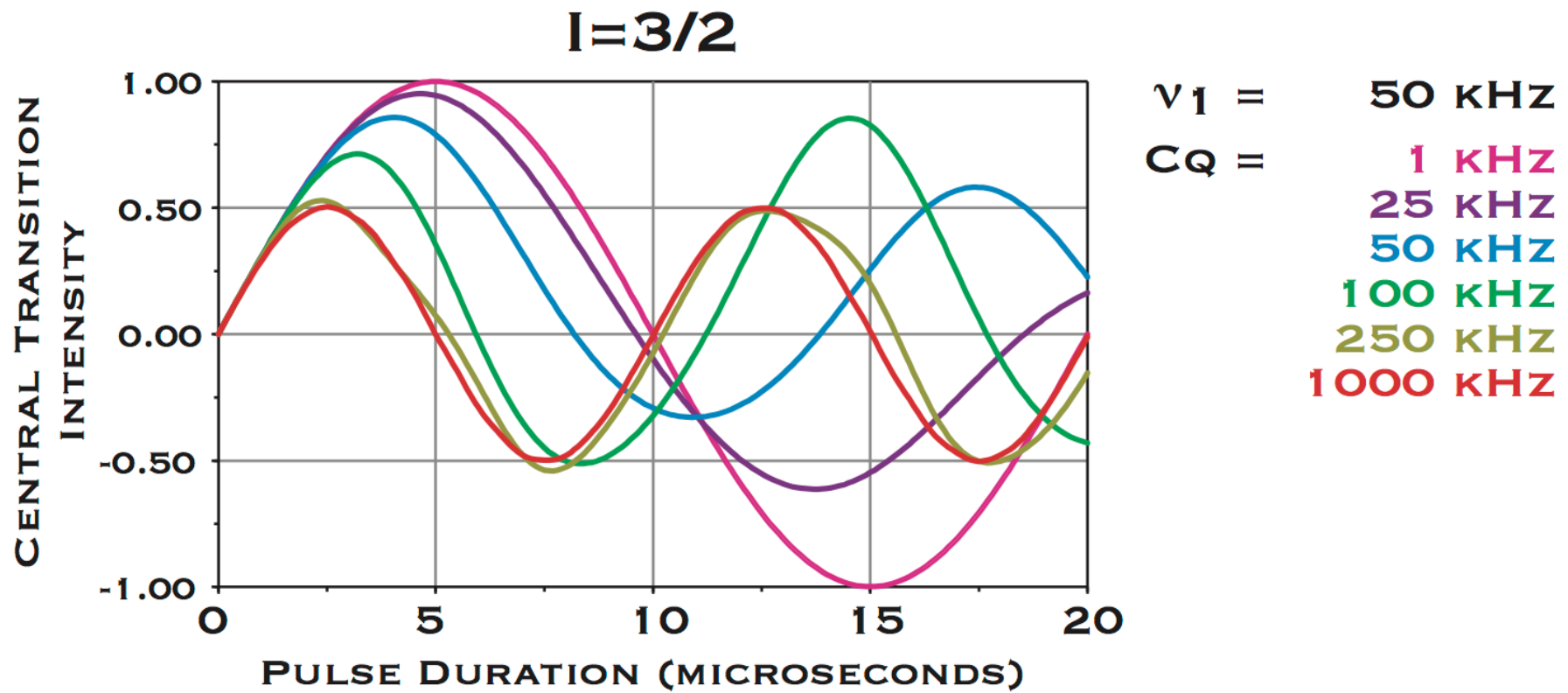
Shifted Echo Data Acquisition and Processing of DAS, MQ-MAS, ST-MAS

J. Magn. Reson. A, 103, 72-81 (1993).



A Few Loose Ends...

Central Transition Nutation Frequency



IN THE LIMIT THAT $\omega_1 \ll \omega_q$ THE EFFECTIVE CENTRAL TRANSITION NUTATION FREQUENCY BECOMES ...

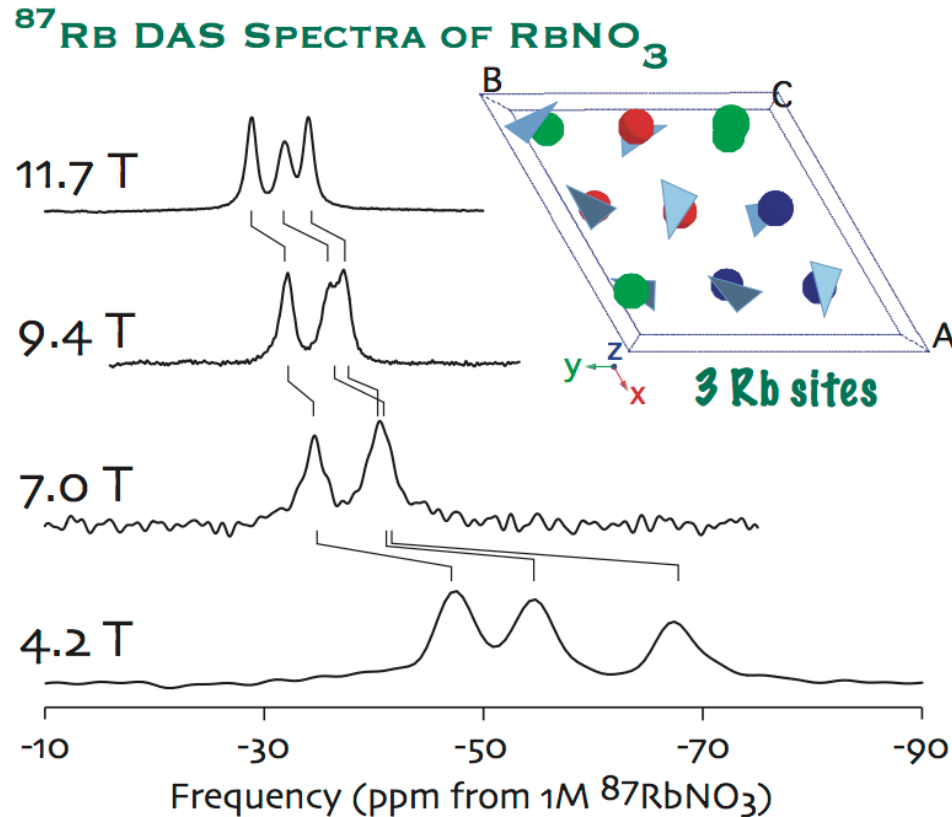
$$(I + 1/2) \omega_1$$

Field Dependence of Isotropic Shift

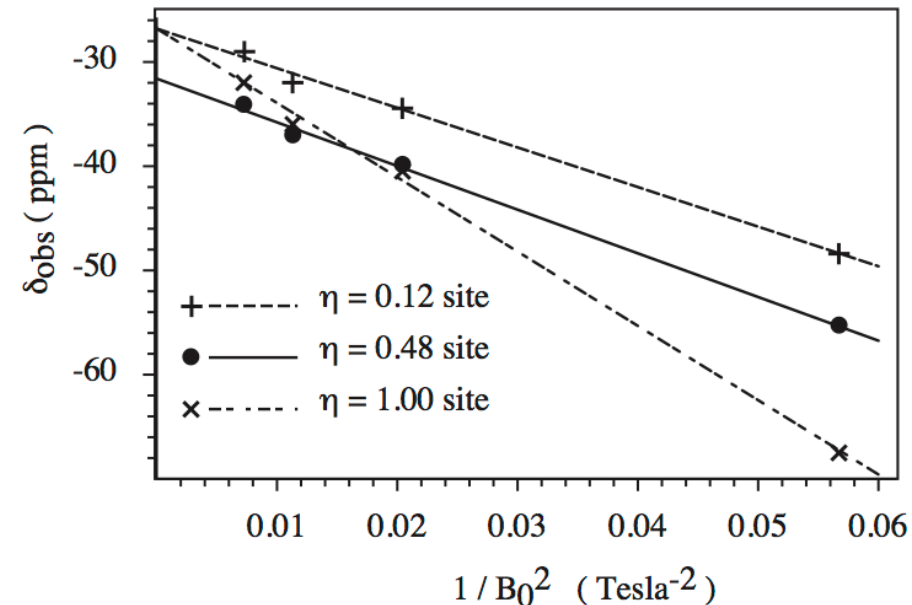
ISOTROPIC FREQUENCY OF QUADRUPOLAR NUCLEUS IS SUM OF ISOTROPIC

- (1) CHEMICAL SHIFT AND
- (2) 2ND ORDER QUADRUPOLAR SHIFT.

$$\Omega^{(iso)} = \delta_{iso}^{(CS)}(\text{ppm}) - \frac{1}{40} \frac{P_q^2}{\nu_0^2} \times 10^6 \text{ (ppm)}$$



$$P_q = C_Q (1 + \eta^2/3)^{1/2}$$

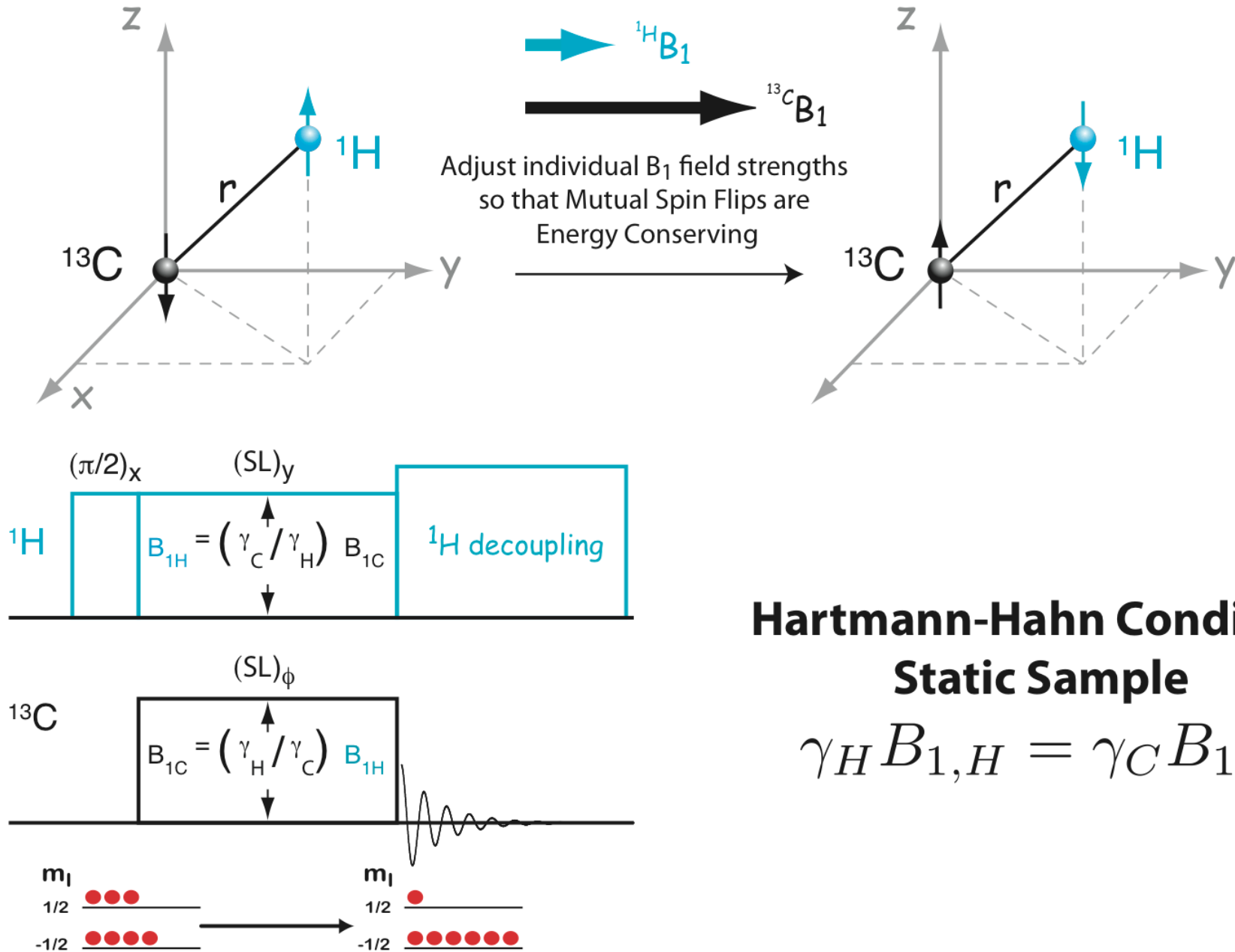


Baltisberger, Gann, Wooten, Chang, Mueller, and Pines, *J. Am. Chem. Soc.*, 1992, **114**, 7489

Warning: Never label spectrum axis of quadrupolar nuclei in Solids as "Chemical Shift". Only true in limit that P_q/ν_0 goes to zero.

Enhancing Sensitivity

Cross-Polarization Transfer: ^1H to ^{13}C



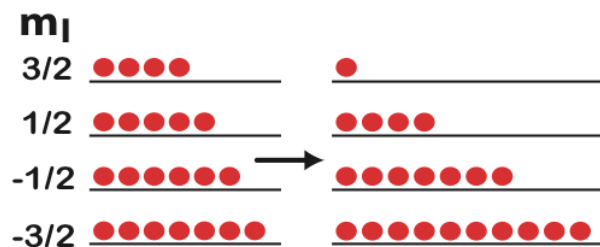
**Hartmann-Hahn Condition
Static Sample**

$$\gamma_H B_{1,H} = \gamma_C B_{1,C}$$

Cross-Polarization Transfer: ^1H to Quadrupole

Hartmann-Hahn Condition when $|\gamma_X B_{1,X}| \gg |\omega_q|$
Static Sample

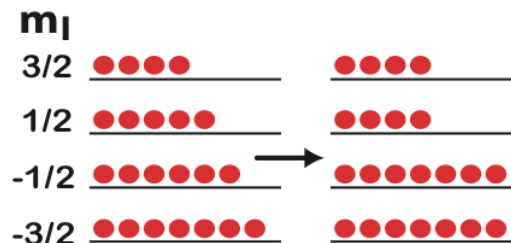
$$\gamma_H B_{1,H} = \gamma_X B_{1,X}$$



All transitions get enhanced polarization

Hartmann-Hahn Condition when $|\gamma_X B_{1,X}| \ll |\omega_q|$
Static Sample

$$\gamma_H B_{1,H} = \left(I + \frac{1}{2} \right) \gamma_X B_{1,X}$$



Only central transition gets enhanced polarization

Cross-Polarization Transfer: ^1H to Quadrupole

Spinning Sample

Hartmann-Hahn Condition when $|\gamma_X B_{1,X}| \gg |\omega_q|$

$$\gamma_H B_{1,H} = \gamma_X B_{1,X} \pm n\Omega_R$$

All transitions get
enhanced polarization



Hartmann-Hahn Condition when $|\gamma_X B_{1,X}| \ll |\omega_q|$

$$\gamma_H B_{1,H} = \left(I + \frac{1}{2} \right) \gamma_X B_{1,X} \pm n\Omega_R$$

Only central transition gets
enhanced polarization

Just like spin 1/2 nuclei the H-H match breaks into spinning sidebands.

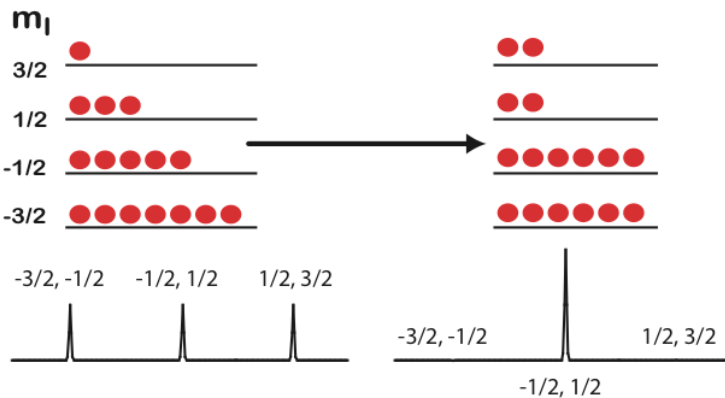
In quadrupolar nuclei, however, level crossings involving central and satellite transitions can further complicate polarization transfer. Check out 2 key papers:

- (1) "MAS NMR Spin Locking of Half-Integer Quadrupolar Nuclei", A. J. Vega, *J. Magn. Reson.* **96**, 50 (1992)
- (2) "CP/MAS of Quadrupolar $S = 3/2$ Nuclei", A. J. Vega, *Solid State NMR*, **96**, 50 (1992)

Population Transfer from Satellites to Central Transition

If you only plan to excite and detection the central transition,
why not steal polarization from the satellites?

Enhance Central Transition by Selective Saturation of Satellite Transitions

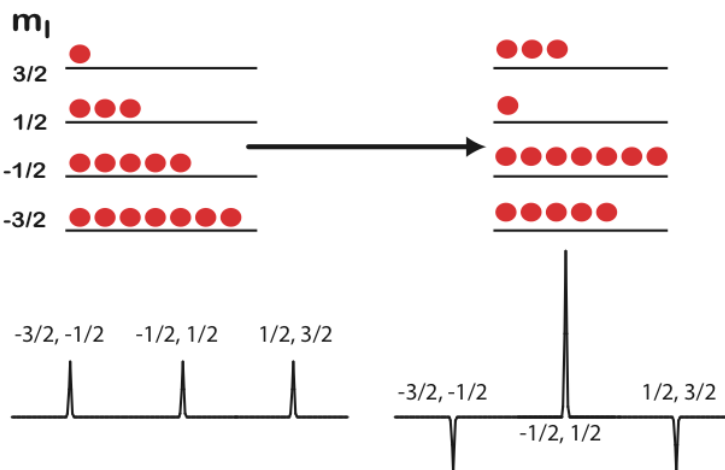


Idea first described by Pound in 1950

Nuclear electric quadrupole interactions in crystals, *Phys. Rev.*, **79**, 685-702 (1950)

If all satellites are saturated the central transition
is enhanced by a factor of $(I+1/2)$

Enhance Central Transition by Selective Inversion of Satellite Transitions



Described by Vega and Naor in 1980.

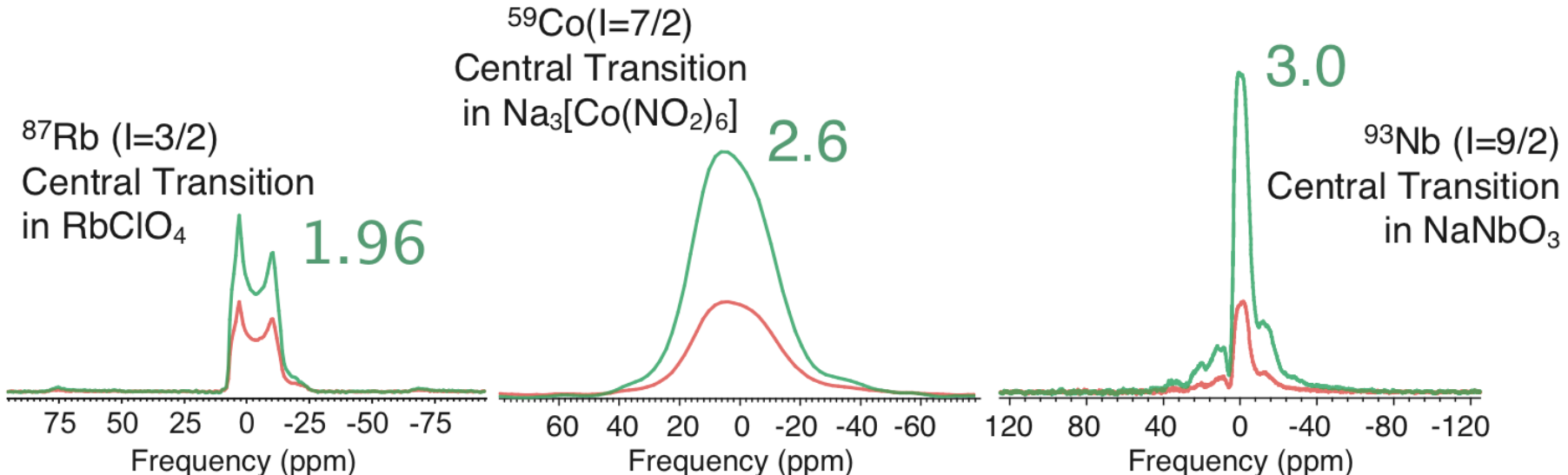
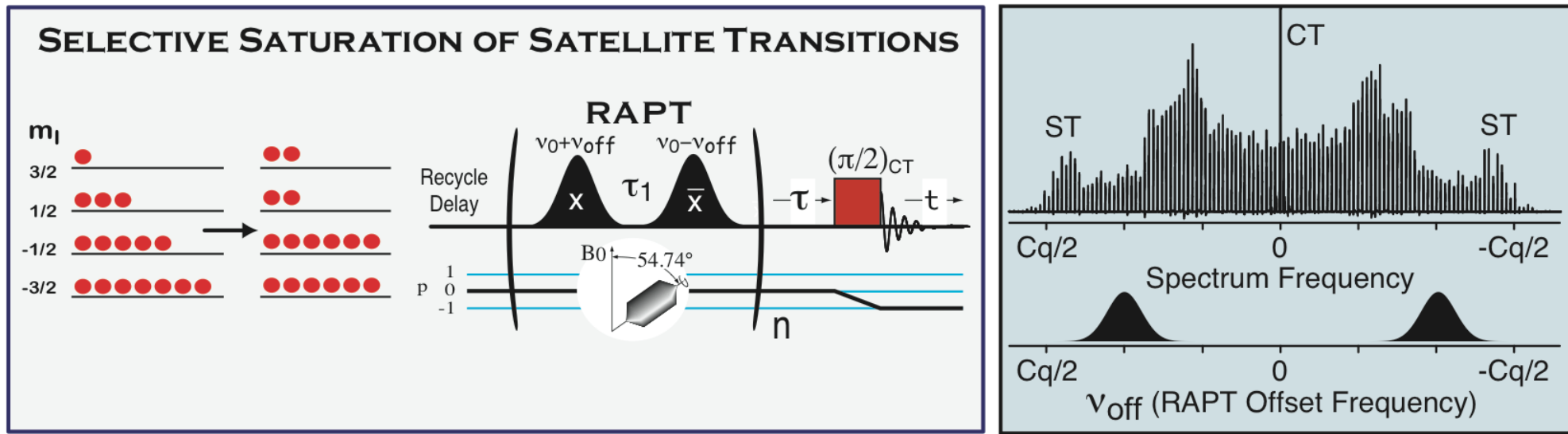
Triple quantum NMR on spin systems with $I=3/2$ in Solids,
J. Chem. Phys., **75**, 75-86 (1981)

If all satellites are inverted (outermost to innermost)
the central transition is enhanced by a factor of $2I$

Rotor Assisted Population Transfer (RAPT) from Satellites to Central Transition

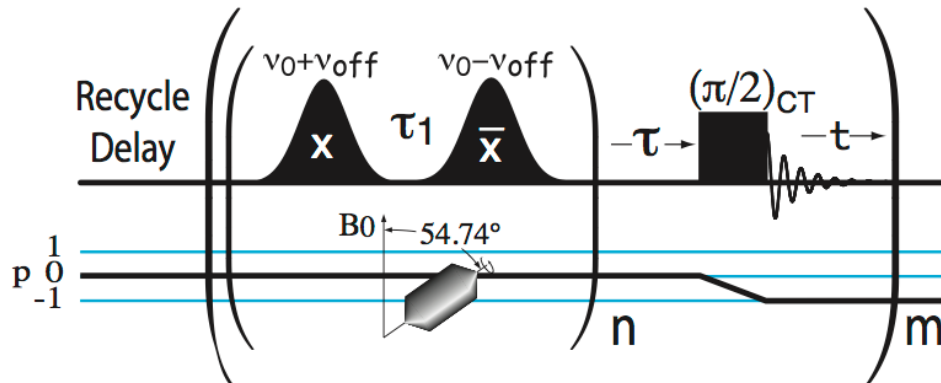
Let the rotor bring the satellites to you

Yao et al., *Chem. Phys. Lett.*, **327**, 85-90 (2000), Prasad et al., *J. Am. Chem. Soc.*, **124**(18), 4964-4965 (2002)



Multiple Rotor Assisted Population Transfers

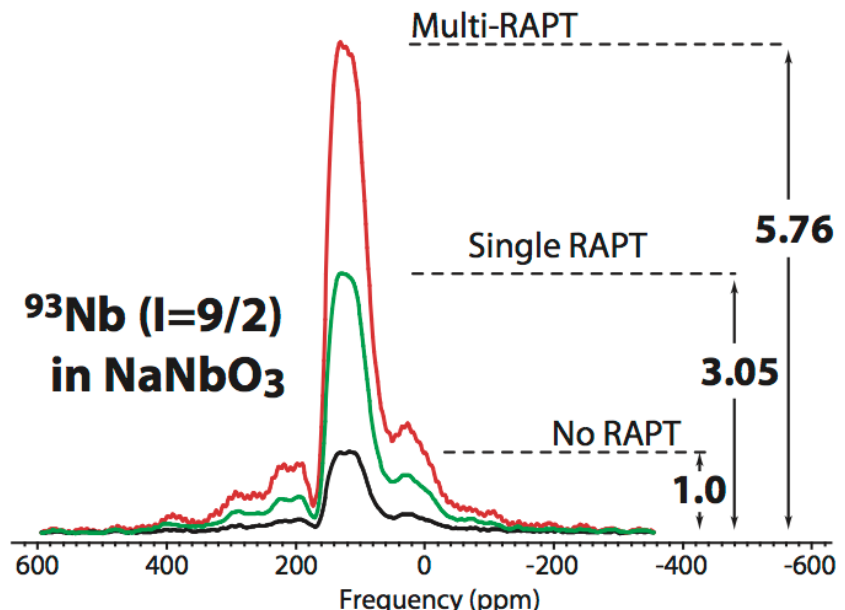
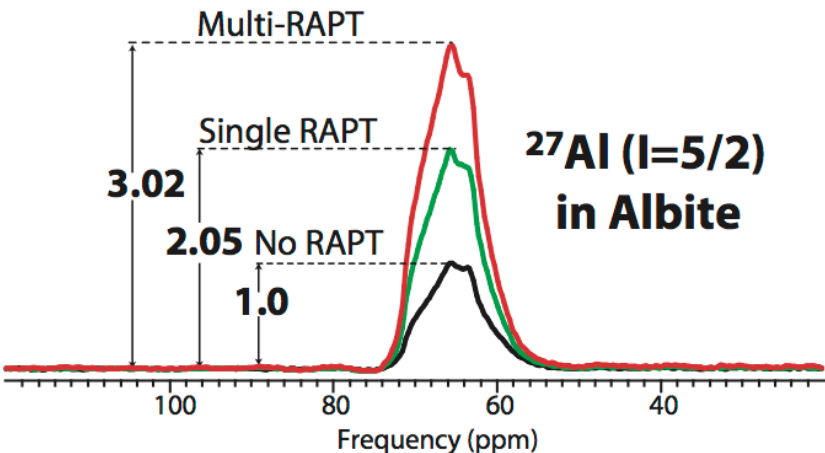
$$\begin{pmatrix} \frac{3}{2} \\ \frac{1}{2} \\ -\frac{1}{2} \\ -\frac{3}{2} \end{pmatrix} \xrightarrow{\text{RAPT}} \begin{pmatrix} 1 \\ 1 \\ -1 \\ -1 \end{pmatrix} \xrightarrow{(\pi/2)_{CT}} \begin{pmatrix} 1 \\ 0 \\ 0 \\ -1 \end{pmatrix} \xrightarrow{\text{RAPT}} \begin{pmatrix} \frac{1}{2} \\ \frac{1}{2} \\ -\frac{1}{2} \\ -\frac{1}{2} \end{pmatrix} \xrightarrow{(\pi/2)_{CT}} \begin{pmatrix} \frac{1}{2} \\ 0 \\ 0 \\ -\frac{1}{2} \end{pmatrix} \xrightarrow{\text{RAPT}} \begin{pmatrix} \frac{1}{4} \\ \frac{1}{4} \\ -\frac{1}{4} \\ -\frac{1}{4} \end{pmatrix} \dots$$



Kwak, et al, Solid-State NMR, 24, 71-77 (2003)

Theoretical gains in sensitivity using RAPT and multiple RAPT

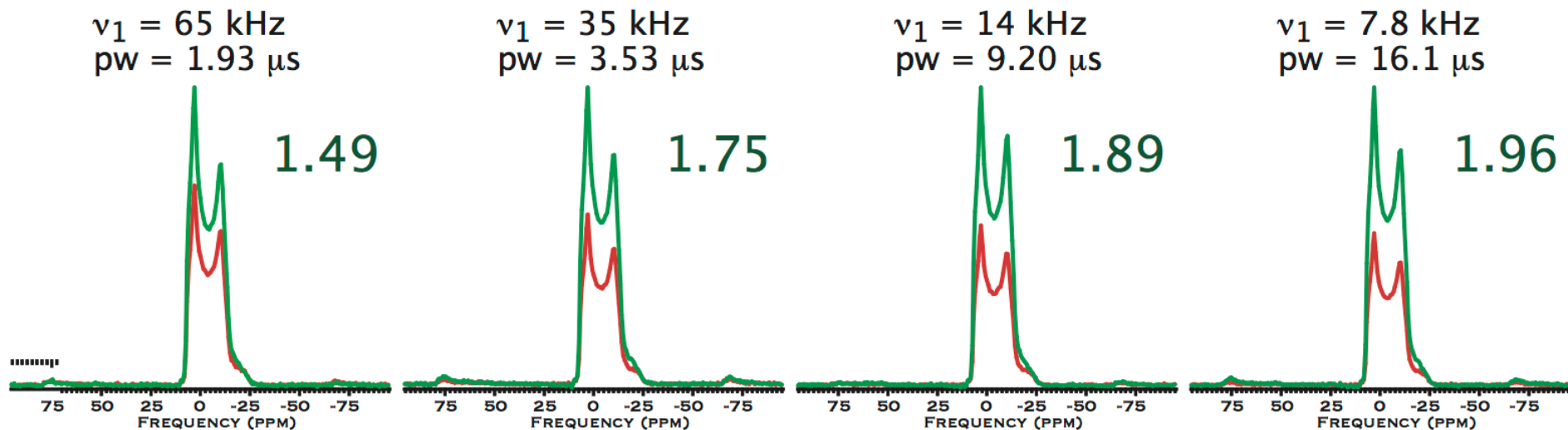
Spin I	Single RAPT Enhancement	Time Reduction	Multi-RAPT Enhancement	Time Reduction
$3/2$	2	4	2.31	5.34
$5/2$	3	9	4.02	16.16
$7/2$	4	16	6.05	36.60
$9/2$	5	25	8.33	69.39



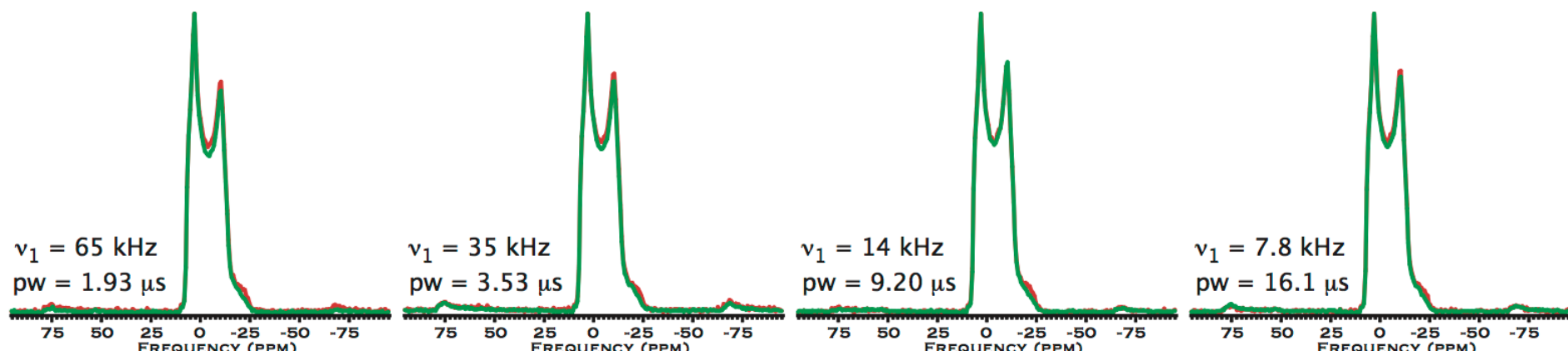
Experimental RAPT Enhanced Spectra (Dependence on Conversion Pulse Power)

^{87}Rb in RbClO_4
RAPT-Saturated Satellites
Equilibrium

Trease et al., *J. Magn. Reson.*, **200**, 334-339 (2009).
Optimum Excitation of Enhanced Central Transition Populations



RAPT SPECTRA SCALED DOWN TO COMPARE LINESHAPES



Pay the Bills...

Interpreting Quadrupolar Couplings (Electric Field Gradients)

$$H_q = \sum_k (-1)^k R_{2k}(\Omega_q) \left[\sqrt{\frac{3}{2}} \frac{eQ\gamma_I}{I(2I-1)} T_{2-k} \right]$$

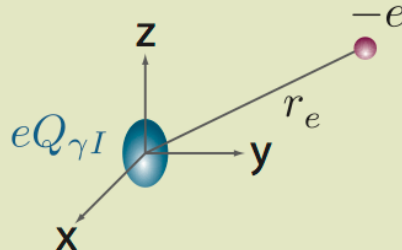
Electric Field Gradient at the nucleus **Nuclear Quadrupole Moment**

Electric Field Gradient at the nucleus

$$R_{2,k} = \sum_{\text{all electrons}} E_{2,k}(e) + \sum_{\text{all nuclei}} N_{2,k}(n)$$

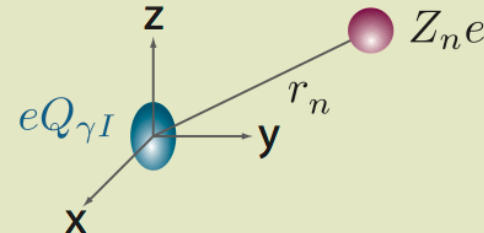
Surrounding Electrons

$$E_{2,k}(e) = -e \sqrt{\frac{4\pi}{5}} \frac{1}{r_e^3} Y_{2,k}(\theta_e, \phi_e)$$



Surrounding Nuclei

$$N_{2,k}(n) = Z_n e \sqrt{\frac{4\pi}{5}} \frac{1}{r_n^3} Y_{2,k}(\theta_n, \phi_n)$$



Total Electric Field Gradient at the Nucleus

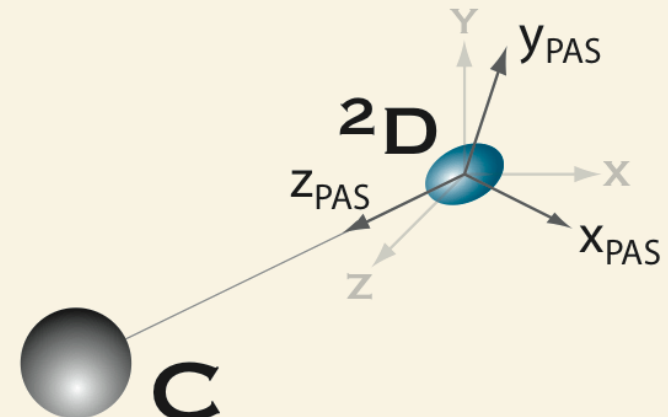
$$\langle R_{2,k} \rangle = \langle \Psi | R_{2,k} | \Psi \rangle$$

Complete nuclear and Electronic Wavefunction

The Electric Field Gradient Tensor and its orientation

- EFG is 2nd rank traceless tensor: 5 elements, $\langle R_{2,k} \rangle$, with $k = -2, -1, 0, 1, 2$.
- There exists a principal axis coordinate system (PAS) where tensor is diagonal: $\langle R_{2,\pm 1}^{\text{PAS}} \rangle = 0$
- Further define PAS such that $|\langle R_{2,0}^{\text{PAS}} \rangle| > |\langle R_{2,\pm 2}^{\text{PAS}} \rangle|$, labeling PAS components as $\langle \rho_{2,k} \rangle \equiv \langle R_{2,k}^{\text{PAS}} \rangle$

For example, in a C-D bond the ²D efg PAS is directed along the C-D bond axis.



- Quadrupolar coupling Constant and Asymmetry parameters are defined

$$C_q = 2 \frac{eQ}{h} \langle \rho_{2,0} \rangle \quad \text{and} \quad \eta_q C_q = 2\sqrt{6} \frac{eQ}{h} \langle \rho_{2,\pm 2} \rangle$$

In Cartesian Coordinates $C_q = e^2 Q \langle q_{zz} \rangle / h$, and $\eta_q = \frac{\langle q_{xx} \rangle - \langle q_{yy} \rangle}{\langle q_{zz} \rangle}$

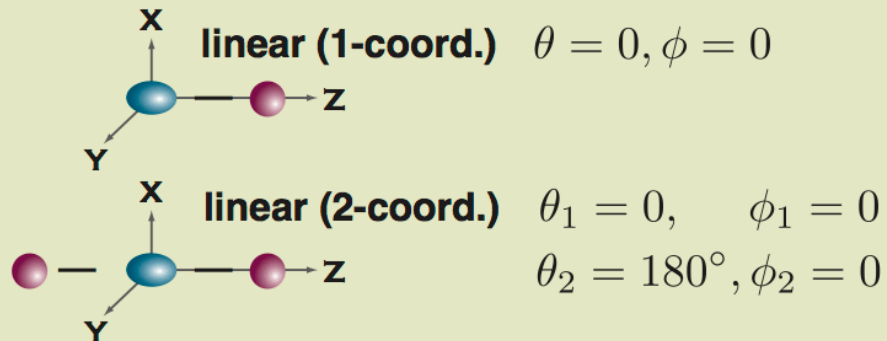
Note that $\langle q_{zz} \rangle + \langle q_{yy} \rangle + \langle q_{xx} \rangle = 0$

Point Charge Model for Predicting Electric Field Gradients

- no analytical expression for EFG exists without approximations.
- most drastic is the Point Charge Model: It's crude, but often provides a qualitative understanding, and with calibration can sometimes be quantitative.

$$\langle R_{2,k} \rangle = \sum_{j=1}^n \frac{Z_j e}{d_i^3} \sqrt{\frac{4\pi}{5}} Y_{2,k}(\theta_j, \phi_j)$$

Approximate coordinating atoms as point charges and calculate sum of all coordinating atoms.



$$\langle R_{2,0} \rangle = \frac{Ze}{d^3}, \quad \langle R_{2,\pm 1} \rangle = 0, \text{ and } \langle R_{2,\pm 2} \rangle = 0$$

$$\langle R_{2,0} \rangle = 2 \frac{Ze}{d^3}, \quad \langle R_{2,\pm 1} \rangle = 0, \text{ and } \langle R_{2,\pm 2} \rangle = 0$$

Point Charge model predicts Cq doubles, and PAS unchanged when atom goes from one to two-coordinated linear.

Experimental ^{17}O NMR measurements in Silicates

Non-Bridging Oxygen Si- $^{17}\text{O}^-$

$\alpha\text{-Na}_2\text{Si}_2\text{O}_5$	$C_q = 2.40 \text{ MHz}$, $\eta = 0.20$
$\text{Li}_2\text{Si}_2\text{O}_5$	$C_q = 2.45 \text{ MHz}$, $\eta = 0.10$

Bridging Oxygen Si- $^{17}\text{O-Si}$

$\alpha\text{-Na}_2\text{Si}_2\text{O}_5$	$C_q = 5.74 \text{ MHz}$, $\eta = 0.20$
$\text{Li}_2\text{Si}_2\text{O}_5$	$C_q = 5.60 \text{ MHz}$, $\eta = 0.10$

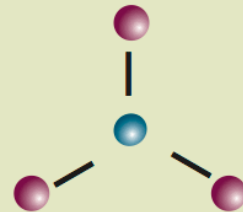
Maekawa, Florian, Massiot, Kiyono, Nakamura, *J. Phys. Chem.* 1996, **100** (17), 5525-5532.

Xue, Stebbins, Kanzaki, *Am. Miner.* 1994, **79**, 31.

Point Charge Model for Predicting Electric Field Gradients

Trigonal Planar

Place quadrupole nucleus at the origin and the z-axis perpendicular to the plane containing 3 point charges

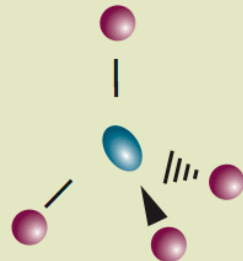


$$\theta = 90^\circ, \phi = 0, \pm 120^\circ$$

$$\langle R_{2,0} \rangle = -\frac{3}{2} \frac{Ze}{d^3}, \quad \langle R_{2,\pm 1} \rangle = 0, \quad \text{and} \quad \langle R_{2,\pm 2} \rangle = 0$$

- z-axis of efg PAS is perpendicular to plane containing nucleus and coordinating charges.
- Asymmetry parameter is zero, and sign of the quadrupole coupling constant is opposite to linear cases.

Tetrahedral



$$\langle R_{2,0} \rangle = 0, \quad \langle R_{2,\pm 1} \rangle = 0, \quad \text{and} \quad \langle R_{2,\pm 2} \rangle = 0$$

^{11}B examples from Borosilicates:

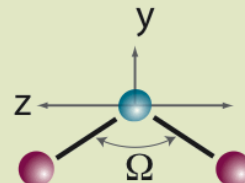
	C_q	η
Trigonal Planar $^{11}\text{BO}_3$ (ring)	2.65 MHz	0.20
Trigonal Planar $^{11}\text{BO}_3$ (non-Ring)	2.55 MHz	0.20
Tetrahedral $^{11}\text{BO}_4$ (1B,3Si)	0.30 MHz	0.00
Tetrahedral $^{11}\text{BO}_4$ (0B 4Si)	0.30 MHz	0.00

Lin-Shu Du and
Jonathan F. Stebbins,
J. Non-Cryst. Solids,
315, 239–255 (2003)

Point Charge Model for Predicting Electric Field Gradients

Bent

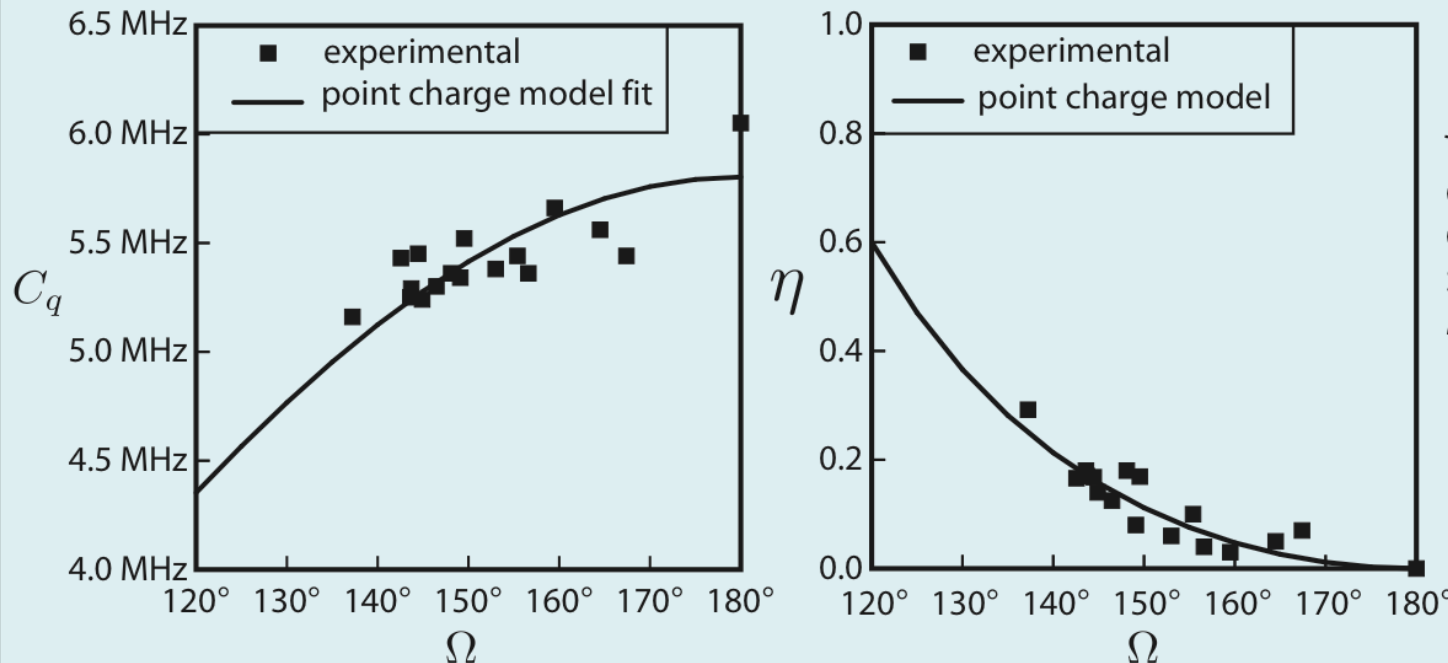
Place quadrupole nucleus at the origin with z-axis in plane containing atoms and perpendicular to the angle bisector



$$\langle R_{2,0} \rangle = \frac{Ze}{d^3} (3 \sin^2 \Omega/2 - 1), \quad \langle R_{2,\pm 1} \rangle = 0, \quad \text{and} \quad \langle R_{2,\pm 2} \rangle = \frac{Ze}{d^3} \sqrt{\frac{3}{2}} \cos^2 \Omega/2$$

$$C_q = 2 \frac{e^2 Q}{h} \frac{Z}{d^3} (1 - \cos \Omega) \quad \text{and} \quad \eta = -\frac{3(\cos \Omega + 1)}{3 \cos \Omega - 1}$$

^{17}O quadrupolar coupling parameters in Si- ^{17}O -Si linkage as a function of Si-O-Si angle



Ferrierite - 10 sites

Bull et al,
J. Am. Chem. Soc., **122**, 4948 (2000)

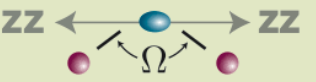
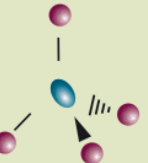
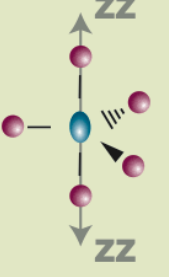
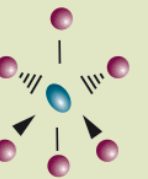
Cristobalite - 1 site

Quartz - 1 site
Spearing et al,
Phys. Chem. Min., **19**, 307 (1992)

Coesite - 5 sites

Grandinetti, et al,
J. Phys. Chem., **99**, 12341 (1995)

Rough Guide to Some Point Charge Models for EFG

Name	Structure	C_q	ηq
linear (1)		$2 \frac{e^2 Q}{h} \frac{Z}{d^3}$	0
linear (2)		$4 \frac{e^2 Q}{h} \frac{Z}{d^3}$	0
bent (2)		$2 \frac{e^2 Q}{h} \frac{Z}{d^3} (1 - \cos \Omega)$	$-\frac{3(\cos \Omega + 1)}{3 \cos \Omega - 1}$
Trigonal Planar (3)		$-3 \frac{e^2 Q}{h} \frac{Z}{d^3}$	0
Tetrahedral (4)		0	0
Trigonal Bipyramidal (5)		$\frac{e^2 Q}{h} \frac{Z}{d^3}$	0
Octahedral (6)		0	0

Acknowledgments

Current Group and Collaborators



Prof. Jay Baltisberger
Berea College



Kevin Sanders



Pyae Phyo, Berea College



Brennan Walder



rmn.grandinetti.org

"Quadrupole" Collaborators

Alex Pines, Jay Baltisberger, Antoine Llor, Margaret Eastman, Young Lee, Boqin Sun, Yue Wu, Jonathan Stebbins, Ian Farnan, Ulrike Werner-Zwanziger, Sheryl Gann, Josef Zwanziger, Joe Sachleben, Maurice Goldman, Zbigniew Olejniczak, Andrew Kolbert, Lucio Frydman, Gerry Chingas, Raz Jelinek, Brad Chmelka, Jacek Klinowski,

Dominique Massiot, Joseph Virlet, Zhehong Gan, Thomas Vosegaard, Lyndon Emsley, Dimitri Sakellariou, Todd Lowary, Michael Deschamps, Franck Fayon, Stefan Steuernagel, Guido Pintacuda

Past Group Members

Prof. Jay Baltisberger
Dr. Pierre Florian
Dr. Alex Klymachyov
Prof. Ted Clark
Dr. Subramanian Prasad
Dr. Mike Davis
Dr. Karl Vermillion
Dr. Ping Zhang
Dr. Hyung-Tae Kwak
Dr. Jason Ash
Dr. Nicole Trease
Dr. Krishna Dey
Zhi Yao
Travis Sefzik
Antonio Paulic
Ramesh Sharma
Derek Kaseman
Kim Shookman
Jacob Sillaman
Eric Keeler
Jason Ezzell
Kevin Sanders
Brennan Walder